Volume 50 / Supplement 107 / 2021

# Vasa

## European Journal of Vascular Medicine



21. Unionstagung der Schweizerischen Gesellschaften für Gefässkrankheiten gemeinsam mit der Schweizerischen Gesellschaft für Ultraschall in der Medizin Sektion Gefässe

21e Congrès de l'Union des Sociétés Suisses des Maladies Vasculaires en collaboration avec la Société Suisse d'Ultrasons en Médecine Section Vaisseaux

**1. – 3. Dezember 2021 | 1 – 3 décembre 2021**
**Interlaken Congress & Events AG**

Union of Vascular Societies of Switzerland
Union Schweizerischer Gesellschaften für Gefässkrankheiten
Union des Sociétés Suisses des Maladies Vasculaires
Unione delle Società Svizzere di malattie vascolari
Uniun da las Societads Svizras da malsognas vascularas
USGG / USSMV www.uvs.ch

hogrefe

# Vasa

European Journal of Vascular Medicine

Volume 50 / Supplement 107 / 2021

## 21. Unionstagung der Schweizerischen Gesellschaften für Gefässkrankheiten gemeinsam mit der Schweizerischen Gesellschaft für Ultraschall in der Medizin Sektion Gefässe

## 21e Congrès de l'Union des Sociétés Suisses des Maladies Vasculaires en collaboration avec la Société Suisse d'Ultrasons en Médecine Section Vaisseaux

**1. – 3. Dezember 2021 | 1 – 3 décembre 2021**
**Interlaken Congress & Events AG**

Meister ConCept GmbH
Bahnhofstrasse 55
5001 Aarau
T +41 62 836 20 90
F +41 62 836 20 97
unionstagung@meister-concept.ch

hogrefe

**Publisher** Hogrefe AG, Länggass-Strasse 76, Postfach CH-3012 Bern, Switzerland, Tel. +41 (0) 31 300 45 00, verlag@hogrefe.ch, www.hogrefe.com/ch/

**Subscriptions** Tel. +41 (0) 31 300 45 55, zeitschriften@hogrefe.ch

**Production** Gerda Schotte, Tel. +41 (0) 31 300 45 78, gerda.schotte@hogrefe.ch

**Frequency** 6 online issues per volume

**Vasa is the official organ of** German Society of Angiology – Society of Vascular Medicine, Swiss Society of Angiology, Slovenian Society of Vascular Diseases, and European Society for Vascular Medicine.

**Vasa is listed in** Medline, Science Citation Index, Expanded (SCIE), SciSearch Current Contents/Clinical Medicine, Science Citation Index, Prous Science Integrity, Journal Citation Reports/Science Edition, Biological Abstracts, BIOSIS Previews, EMBASE, and Scopus.

Library of Congress Catalog Card Number 72-96 773

**Impact Factor** 1.961 (Journal Citation Reports 2020 SCI, © Clarivate Analytics 2021)

**H Index** 36

**Prices** *Subscription rates per year:*
Libraries/Institutions: from CHF 505.– / € 427.– / US $ 490.– (Prices depend on the size of the institution and can be found can be found in our journals catalogue: hgf.io/zftkatalog)

Individuals: CHF 172.– / € 128.– / US $ 159.–

*Single Issue:* CHF 74.– / € 55.– / US $ 69.–

Vasa is available online only.



ISSN-L 0301-1526
ISSN 0301-1526 (Print)
ISSN 1664-2872 (online)

# Themenübersicht / Aperçu des thèmes

 

# Angiology

## FM 1.1

### Effects of three versus five times per week treadmill exercise training on walking capacity and expression of genes related to glucose metabolism in a mouse model of lower extremity peripheral artery disease

*J. Lavier, K. Bouzourène, G. Millet, N. Rosenblatt-Velin, L. Mazzolai, M. Pellegrin (Lausanne)*

**Objective:** Lower extremity peripheral artery disease (PAD) is a major health issue in Switzerland. Treadmill exercise is an essential therapeutic strategy for PAD, however underlying adaptations in lower extremity skeletal muscle remain unclear. The present study examined the effects of three versus five times per week exercise training on walking capacity and muscular expression of glucose metabolic genes in a mouse model of PAD.
**Methods:** Hypercholesterolemic Apolipoprotein E-deficient mice with right hindlimb ischemia were divided into three groups: sedentary (SED), three times per week exercise (3x-EX), and five times per week exercise (n=5x-EX). Mice were trained at moderate intensity for 7 weeks. Maximal walking distance was determined using an incremental treadmill test. Glucose metabolism-related gene expression in ischemic and non-ischemic gastrocnemius muscles was examined by quantitative RT-PCR.
**Results:** Maximal walking distance was improved to the same extent in mice following three (+58%, $p<0.05$) or five (+82%, $p<0.01$) times a week treadmill exercise while no improvement was observed in SED mice. Expression of glucose transporter isoform 1 (GLUT-1) and hexokinase 2 (HK2) was decreased in the ischemic and non-ischemic muscles, both in 3x-EX and 5x-EX compared to SED ($p<0.05$). Phosphofructokinase (PFK) expression was only decreased in the non-ischemic muscle of both exercised groups ($p<0.05$ vs. SED). Glycogen synthase 1 (GYS1) and pyruvate dehydrogenase kinase 4 (PDK4) expression levels were increased only in the ischemic muscle of both exercised groups compared to their respective non-ischemic muscles ($p<0.05$). 3x-EX and 5x-EX decreased expression of lactate dehydrogenase A (LDH-A) in the non-ischemic muscle ($p=0.09$ and $p<0.05$ vs. SED, respectively) and expression of lactate dehydrogenase B (LDH-B) both in the non-ischemic and ischemic muscles ($p<0.01$ vs. SED). Moreover, 5x-EX decreased monocarboxylate transporter 1 (MCT1) expression both in the ischemic and non-ischemic muscles ($p<0.05$ vs. SED), while 3x-Ex decreased MCT1 expression in the ischemic muscle only ($p<0.05$ vs. SED).
**Conclusion:** Treadmill exercise three or five times a week are equally effective in improving walking capacity in a PAD mouse model. Exercise modulates muscular expression of genes regulating glucose transport, glycolysis, and lactate metabolism.

## FM 1.2

### Daily ultrasound screening in critical stage SARS-CoV-2 patients to detect high risk for venous thromboembolism

*G. Prouse[1], L. Ettorre[1], J.C. Van den Berg[1], L. Spinedi[2], F. Riva[1], L. Giovannacci[1] ([1]Lugano, [2]Locarno)*

**Objective:** A reliable deep venous thrombosis (DVT) indicator in critical patients with SARS-CoV-2 has not yet been identified and could be used to determine the best antithrombotic strategy. Different studies have shown some conflicting evidence about the safety and effectiveness of therapeutic anticoagulation versus regular or higher intensity thromboprophylaxis in critical COVID-19 patients. The aim of our study was to most accurately determine the incidence of DVT in this subset of SARS-CoV-2 patients and to search for a reliable tool to identify those who might benefit from therapeutic anticoagulation.
**Methods:** From March 1, 2020 to May 31, 2020, all patients admitted to the intensive care unit for SARS-CoV-2 were prospectively enrolled and screened daily with ultrasound for DVT. A higher-intensity thromboprophylaxis regimen was adopted in all patients that where not at high risk for bleeding. Sepsis-induced coagulopathy (SIC) and sequential organ failure assessment (SOFA) scores were analyzed with a time-to-DVT event in a COX proportional-hazard regression model. Receiver operating characteristic (ROC) curves were used to determine sensitivity and specificity and the Youden's Index to find the most useful threshold.
**Results:** 96 patients were enrolled and DVT was detected in 37% of them. SIC and SOFA scores were both correlated to DVT. A SIC score of 1 vs ≥2 showed a close association with DVT, but most significantly a SOFA score of 1 or 2 points was most accurate in predicting the absence of DVT, indicating a therapeutic anticoagulation is likely unnecessary in these patients. Its sensitivity, specificity, and positive and negative predictive values were 87.9%, 100%, and 100% and 93.7%, respectively. D-dimer displayed a significantly lower sensitivity and platelet count and aPTT were not found to be correlated to DVT.
**Conclusion:** Critical patients with SOFA scores of 1 or 2 are at low risk of developing DVT and are unlikely to benefit from therapeutic-intensity anticoagulation. Conversely, patients with scores ≥3 are at high risk for DVT and may represent a subgroup that could benefit from therapeutic anticoagulation.

## FM 1.3

### The C-type Natriuretic peptide: a new player in the development of the Marfan syndrome ?

*S. Clerc Rignault, C. Bielmann, S. Déglise, K. Bouzourene, L. Mazzolai, N. Rosenblatt-Velin (Lausanne)*

**Objective:** Marfan Syndrome (MFS) is an autosomal dominant inherited connective tissue disorder affecting the cardio-vascular system. Aortic dissections and ruptures are the primary cause of morbidity and mortality in these patients. No treatment really cures patients.
The C-type natriuretic peptide (CNP) is a local regulator of skeletal growth and of vascular homeostasis, remodeling and angiogenesis.



https://doi.org/10.1024/0301-1526/a000973

CNP is constitutively released by endothelial cells, whereas TGF beta (increased in Marfan patients) stimulates its secretion by smooth muscle cells.

The aim of this project is to determine whether altered CNP signaling pathway contributes to the development of the vascular phenotype in MFS.

**Methods:** Plasma and vessel biopsies will be taken from Marfan patients (RAVAD registery, CHUV Lausanne). Only patients with Marfan syndrome due to the Fibrillin1 mutation (genetic diagnosis) were selected. Experiments will be also performed on Fbn1 C1041G/+ mouse model which recapitulates several of the human phenotypes, including aortic wall degeneration and aneurysm development. proCNP and CNP concentrations will be determined in the plasma of humans and mice suffering from MFS. The protein levels of proCNP, CNP and of its receptors, NPR-B and NPR-C, will be evaluated by Western blot analysis in aortic tissue during the development of MFS.

**Results:** proCNP level was decreased in Marfan patients compared to age and sex-matched non Marfan patients (18 pmol/l versus 310; p=0.07). However, proCNP processing was similar in Marfan and non Marfan patients as shown by the level of NT-proCNP (30 versus 22 pmol/l).

In 6–7 week-old male Fbn1 C1041G/+ mice, CNP protein levels are 1.6 and 4.0-fold increased in aortic arch and thoracic aorta, respectively. NPR-B and NPR-C protein levels remained unchanged. No difference was found in female mice. In 24 week-old Marfan male mice , CNP protein level is normalized in aortic arch but decreased in thoracic aorta (–34%). NPR-C protein level is 2-fold decreased in the aortic arch and ascending and thoracic aorta.

**Conclusion:** Progression of Marfan disease in the aortic arch and ascending and thoracic aortas in mice is associated with changes of the level of CNP and NPR-C proteins. These results will help to understand the role of the CNP-mediated signaling pathway in the development of MFS and could open the door to new therapies for patients.

## FM 1.4

## Exercise-induced Angiogenesis is Dependent on Metabolically Primed Atf3/4+ Endothelial Cells

*Z. Fan (Schwerzenbach)*

**Objective:** Exercise is one of the very few conditions in adulthood during which physiological angiogenesis takes place, but mechanisms through which exercise promotes angiogenesis are poorly understood.

**Methods:** Using single cell RNAseq experiments, functional angiogenic and metabolic assays and genetic mouse models.

**Results:** We showed that exercise-induced angiogenesis is executed by a subpopulation of capillary endothelial cells (ECs) which is characterized by the differential expression of atf3/4. We found that atf3/4+ and atf3/4- capillary ECs are not only transcriptionally distinct, but are spatially located within a different microenvironment. Atf3/4+ ECs are juxtaposed red oxidative fibers (=red muscle ECs or RmECs) whereas atf3/4- ECs are juxtaposed white glycolytic fibers (=white muscle ECs or WmECs). Thus, angiodiversity in muscle shows spatial differences which are defined by the metabolic microenvironment. Upon isolation and culture, WmECs have impaired angiogenic potential when compared to RmECs through reduced proliferation. Mechanistically, we show that atf3/4 limit the ability of the angiogenic masterswitch cMYC, which controls EC metabolism and growth, to transcriptionally activate a broad amino acid metabolic reprogramming that supports endothelial growth and proliferation. When compared to RmECs, we found that WmECs have reduced expresssion of genes involved in amino acid uptake and metabolism. As a consequence, WmECs (and atf3/4KD cells) take up less amino acids and have lower ability to de novo synthesize amino acids (such as serine and glycine) leading to a significant reduction in intracellular amino acid levels. Thus, we show that ATF3/4 metabolically prime RmECs for angiogenesis and identify metabolic angiodiversity as a crucial predictor of angiogenic capacity in muscle. We provide in vivo evidence for our hypothesis by showing that exercise-induced angiogenesis selectively occurs within the oxidative areas where atf3/4+ capillary ECs reside. Finally, endothelial specific deletion of atf4 confirmed that exercise-induced angiogenesis is dependent on atf4.

**Conclusion:** Taken together, our data highlight that metabolic priming of endothelial cell subpopulations by atf3/4 in the muscle defines their angiogenesis potential.

## FM 1.5

## Descending stair walking in patients with symptomatic lower extremity peripheral artery disease: a promising new exercise modality

*S. Lanzi, P. Nussbaumer, L. Calanca, L. Mazzolai, D. Malatesta (Lausanne)*

**Objective:** This study aimed to compare cardiovascular and muscular acute responses of descending (DSW) and ascending (ASW) stair walking in patients with symptomatic lower extremity peripheral artery disease (PAD).

**Methods:** Patients randomly performed DSW and ASW exercise sessions (matched for mechanical work) consisting in 6 repetitions of two min effort interspersed with two min recovery. At the end of each repetition, heart rate (HR), systolic blood pressure (SBP), rate of perceived exertion (RPE), calf muscle oxygen saturation ($StO_2$), and claudication pain were assessed. Plantar flexion maximal voluntary isometric contraction (MVC-iso) was measured pre-, post-, and 48h post-exercise. Delayed-onset muscle soreness (DOMS) was assessed at 24h, 48h, and 72h post-exercise. Perceived enjoyment of the training sessions were also recorded.

**Results:** Nine symptomatic patients with chronic Fontaine stage II PAD were included (62.0±2.4 yr; ankle-brachial index 0.77±0.05). Compared to ASW, DSW elicited a significantly lower HR (–17%, P≤0.001), SBP (–18%, P≤0.001), RPE (–30%, P≤0.001), calf muscle desaturation (–11%, P≤0.001), and claudication pain (–60%, P≤0.001). DSW was significantly more appreciated (+16%, P=0.02). Compared to post-ASW, MVC-iso was significantly lower 48h post-DSW (–8%, P=0.03). In addition, DOMS was significantly higher following DSW session (main effect over the three time points: +76%; P=0.035).

**Conclusion:** At matched mechanical work, DSW elicited lower cardiovascular response and calf muscle desaturation compared to ASW in symptomatic patients with chronic PAD. DSW was associated with decreased claudication pain, likely contributing to greater perceived

exercise enjoyment. Introduced progressively in training programs to minimize muscle damage, DSW may be a promising and complementary training modality to optimize health-related outcomes in patients with symptomatic PAD. Further studies are however needed to determine benefit of DSW on walking impairment in chronic PAD.

## FM 1.6

### Association of sex and cardiovascular risk factors with atherosclerosis distribution pattern in lower extremity peripheral artery disease

*O. Baretella, L. Buser, C. Strametz, D. Häberli, A. Lenz, Y. Döring, I. Baumgartner, M. Schindewolf (Bern)*

**Objective:** Atherosclerosis expression varies across coronary, cerebrovascular and peripheral arteries, but also within the peripheral vascular tree. The underlying pathomechanisms of distinct atherosclerosis phenotypes in lower extremity peripheral artery disease (LEAD) is poorly understood.
**Methods:** In a cross-sectional analysis of >15.000 patients undergoing first-time endovascular recanalisation for symptomatic LEAD, data of patients with extreme anatomic phenotypes of either proximal (iliac) or distal (infrageniculate) atherosclerosis were extracted. We performed a multivariate logistic regression model with backward elimination to investigate the association of proximal and distal LEAD with CVRFs.
**Results:** Of 637 patients (29 % women) with endovascular recanalisation, 351 (55%) had proximal, 286 (45%) distal atherosclerosis. Female sex (OR 0·33, 95%CI 0·20 to 0·54), P =0·01), active smoking (OR 0·16, 95%CI 0·09 to 0·28), P <0·001, and former smoking (OR 0·33, 95%CI 0·20 to 0·57, P <0·001) were associated with proximal disease. Diabetes mellitus (DM) (OR 0·33, 95%CI 1·06 to 1·61 P =0·01), chronic kidney disease (CKD) (OR 1·18, 95%CI 1·08 to 1·28), p<0·001), and older age (OR 1·31, 95%CI 1·06 to1·61), P =0·01) were associated with distal disease.
**Conclusion:** Female sex, particularly in the context of smoking, is associated with clinically relevant, proximal atherosclerosis expression. Our additional findings that distal atherosclerosis expression is associated with DM, CKD and older age suggest that LEAD has at least two distinct atherosclerotic phenotypes with sex-specific and individual susceptibility to atherogenic risk factors.

## FM 1

### Clinical presentation of simple and combined or syndromic arteriovenous malformations

*S.M. Bernhard, A. Tuleja, J.E. Laine, F. Haupt, D. Häberli, U. Hügel, J. Rössler, M. Schindewolf, I. Baumgartner (Bern)*

**Objective:** Arteriovenous malformations of the lower extremities (AVM-LE) can present in simple and complex combined or syndromic form (e.g. Parkes Weber Syndrome). We aimed to characterize differences in clinical presentation and course of these potentially life and limb threatening congenital vascular malformations.
**Methods:** We conducted a retrospective analysis of a consecutive series of patients with AVM-LE, who presented in a tertiary referral center in Switzerland between 2008 and 2018. Clinical baseline characteristics, D-dimer level and course were summarized and differences between simple, non-syndromic and combined or syndromic AVM-LE calculated. Odds ratios (OR) and 95% confidence intervals (CI) were estimated using logistic regression models.
**Results:** Overall, we had 506 patients in our congenital vascular malformation registry, 31 (6%) with AVM-LE. There were 16 women and 15 men with a mean age of 18 years at first diagnosis (1 month – 72 years). Simple AVM-LE was present in 22 (71%), combined or syndromic AVM-LE with limb overgrowth in 9 patients (29%), respectively. Common symptoms and signs were pain 25 (81%), swelling 21 (68%) and soft tissue hypertrophy 13 (42%). Among combined or syndromic patients, 3 patients died from wound infection with sepsis and disseminated intravascular coagulation with bleeding complications in form of intracranial hemorrhage and bleeding from extensive leg ulcers. Combined or syndromic patients presented more often with bleeding (67% vs. 5%; p<0.001), malformation related infection (44% vs. 5%; p=0,017) and leg length difference (56% vs. 14%; p=0.049). D-dimer levels were elevated (mean 17256 µg/L, range 1557 µg/L to 80000 µg/L) and angiographic appearance showed complex, mixed type of AVMs, including interstitial type IV, in all patients with combined or syndromic AVM-LE.
**Conclusion:** Patients with congenital simple AVM-LE often present with benign clinical features and are rarely seen with complications related to hemodynamic changes. Patients with combined or syndromic AVM-LE often face serious complications dominated by other than direct high flow related heart failure.

## FM 2

### Outcome after bilateral deep vein thrombosis

*A. Fürbringer[1], M. Janscak[1], C. Jeanneret-Gris[2] ([1] Basel, [2]Bruderholz)*

**Objective:** So far, the outcome after bilateral deep vein thrombosis (DVT) compared to unilateral DVT has not yet been well researched, although a difference would provide important information for diagnostics as well as procedures. The aim of the study was to assess how often DVT occurs bilaterally and if this has an impact on the recurrence rate of thromboembolic disease and of the development of malignant tumors. Additionally, baseline information of patients with bilateral DVT and its outcome was investigated.
**Methods:** For this observational study, we retrospectively screened all patients examined in one hospital from 2000 until 2017 for diagnosed DVT. Of these patients (n = 2409), the history of DVT was assessed and they received a follow-up questionnaire to investigate whether they suffered recurrences or developed malignant tumors. 755 patients were included in the follow-up cohort (604 with unilateral, 151 with bilateral DVT). We performed nonparametric tests to assess two group analysis.
**Results:** The evaluation revealed that patients with bilateral DVT develop significantly more cancer either at time of diagnosis or in the course than patients suffering from unilateral DVT (22.5% vs. 15.4%, p = 0.036). They also endure significantly more often pulmonary embolism simultaneously (33.8% vs. 20.8%, p < 0.001). Patients with bilateral DVT were found significantly older (Mdn = 69) than patients



 

with unilateral DVT (Mdn = 63, p < 0.001). In addition, patients with bilateral DVT show higher mortality (9.1% vs. 5.2%, p = 0.002). A correlation between bilateral DVT and a higher recurrence rate could not be observed.

**Conclusion:** Due to the findings of our studies, we recommend screening patients with bilateral DVT more accurately for concurrent pulmonary embolism and malignant tumors. If the DVT was unprovoked and no tumor is found, the patient should be monitored over the upcoming years to detect a potentially developing malignant tumor.

## FM 3

### Catheter-directed thrombolysis for coronavirus disease 2019 (COVID-19)-associated acute pulmonary embolism: a case-control study

*D. Voci, S. Zbinden, E. Micieli, T. Sebastian, N. Kucher, S. Barco (Zürich)*

**Objective:** Ultrasound-assisted catheter-directed thrombolysis (CDT) can improve hemodynamic parameters in patients with acute pulmonary embolism (PE) and right ventricular dysfunction. The rate of bleeding complications associated with CDT appears to be lower compared with systemic thrombolysis. Only sparse data on the use of CDT for coronavirus disease 2019 (COVID-19)-associated acute PE are available.

**Methods:** We screened all patients with an established diagnosis of intermediate-high/high-risk acute PE, who were treated with ultrasound-assisted-CDT (EKOS, Boston Scientific, US), 2018–2021. We identified 9 patients hospitalized for COVID-19 and 27 age-sex matched controls without COVID-19. The following study outcomes have been prespecified in the study protocol approved by the ethical commission before data collection: (i) mean pulmonary arterial pressure (mPAP) before and at the end of CDT; (ii) hemodynamic decompensation and mortality within 7 and 30 days of treatment; (iv) other complications (PE recurrence, major bleeding, stroke, device-related complications) within 30 days of treatment. Standard informed consent was provided.

**Results:** Of 36 patients 24 (66.7%) were men and the mean age was 67 (SD 14) years (Table I). All patients received anti-Xa activity-adjusted unfractionated heparin and a total of 10 to 20 mg recombinant tissue plasminogen activator over 15 hours. Among COVID-19 patients, mPAP decreased from a mean of 32.3 (SD 8.3) to 22.4 (7.0) mmHg (absolute difference 9.9 mmHg; 95%CI 2.2–17.6). Among non-COVID-19 patients, mPAP decreased from a mean of 35.4 (SD 9.8) to 24.1 (7.0) mmHg (absolute risk difference 11.3 mmHg; 95%CI 6.7–16.0). The mean mPAP reduction did not statistically differ between groups. One patient with COVID-19 died because of COVID-19-related complications (pneumonia, sepsis, multiorgan failure) 14 days after the diagnosis of acute PE. No deaths were recorded among non-COVID-19 patients within 30 days of hospitalization. No recurrent PE events were recorded in both groups within 30 days of hospitalization. One patient in the non-COVID-19 group had a recurrent PE event 6 weeks after index PE. No major bleeding events, strokes, or device-related complications were observed.

**Conclusion:** CDT rapidly reduced the mean pulmonary arterial pressure in acute PE patients with COVID-19. This reduction was similar to that observed among non-COVID-19 patients.

**Table I.** Baseline characteristics of the study population

| | COVID-19 patients (n=9) | Non-COVID-19 patients (n=27) |
|---|---|---|
| Age (years), mean (SD) | 67.7 (13.9) | 67.3 (13.8) |
| Men, n (%) | 6 (66.7) | 18 (66.7) |
| Body Mass Index (kg/m2), mean (SD) | 27.1 (3.8) | 29.5 (6.9) |
| PE upon or during hospitalization, n (%) | 4 (44.4) | 6 (22.2) |
| Deep vein thrombosis, n (%) | 1 (11.1) | 7 (25.9) |
| RV/LV ratio, mean (SD) | 1.50 (0.36) | 1.27 (0.11) |
| PE location, n (%) | Central: 9 (100)<br>Bilateral: 9 (100) | Central: 26 (96.3)<br>Bilateral: 25 (92.6) |
| Troponin I (ng/ml), mean (SD) | 165 (145) | 102 (88) |

## FM 5

### Unravelling the role of vascular ChemR23 expression in atherosclerosis

*B. Evans[1], Y. Yan[2], E. van der Vorst[2,3,4], S. Gencer[2], Y. Jansen[2], T. Thakur[1], N. Angliker[1], M. Siegrist[1], C. Weber[2], I. Baumgartner[1], Y. Döring[1,2], ([1]Bern, [2]Munich DE, [3]Maastricht NL, [4]Aachen DE)*

**Objective:** Our published work showed that hematopoietic deficiency of the chemokine like receptor ChemR23 increases the proportion of alternatively activated M2 macrophages and attenuates pDC recruitment to lymphatic organs and atherosclerotic lesions, in murine models. This synergistically restricts atherosclerotic lesion progression. However, conflicting results in systemic ChemR23-deficient animals suggests ChemR23 has a diverse role within atherosclerosis. Therefore, we investigated the role of ChemR23 on arterial endothelial and smooth muscle cells.

**Methods:** Using our knock out/knock in reporter mouse we performed a bone marrow transplantation, transplanting Apoe-/- bone marrow into Apoe-/- and Apoe-/-ChemR23eGFP/eGFP mice respectively. Mice were fed a Western diet (WD) for 6 or 12 weeks. To further unravel phenotypic consequences of ChemR23 deficiency on vascular endothelial (EC) and smooth muscle cells (VSMC) we performed immunohistochemial stainings and mRNA expression analysis in aortic arches and aortic roots of animals lacking somatic ChemR23 and Apoe-/- control mice. In parallel, human EC/VSMCs will be cultured in vitro in absence and presence of different ligands (e.g. resolvin E1 and chemerin variants), with and without ChemR23 inhibition. This will identify the key signaling pathways of ChemR23 which mediating either a pro- or anti-inflammatory responses.

**Results:** Initial hematoxylin and eosin staining demonstrated that a lack of ChemR23 on somatic cells, resulted in a significantly increased lesion sizes but no increase in macrophage infiltration. Instead an increase in smooth muscle cells in the plaques of Apoe-/- into Apoe-/-ChemR23eGFP/eGFP mice was observed for both at 6 and 12 weeks. Of note, neither pDC and monocyte frequencies, plasma cholesterol, triglycerides nor chemerin levels were affected. Further staining for smooth muscle actin and Nile red highlighted an increase in smooth muscle derived foam cells in the plaques of mice were ChemR23 was lost.

**Conclusion:** Our novel data points at an atheroprotective role of somatic -most likely vascular- ChemR23 expression, suggesting that ChemR23 orchestrates an anti-inflammatory response in vascular endothelial and smooth muscle cells.

**FM 6**

## Impact of popliteal vein thrombosis on clinical and duplex sonographic outcomes in patients with acute iliofemoral deep vein thrombosis treated with endovascular early thrombus removal

*V. Frey[1], T. Sebastian[2], S. Barco[2], D. Spirk[3], D. Hayoz[1], D. Périard[1,2], N. Kucher[2], D. Betticher[1], R. Engelberger[1] ([1]Fribourg, [2]Zürich, [3]Bern)*

**Objective:** Catheter-based thrombus removal (CBTR) as compared to anticoagulation therapy alone reduces the risk of developing moderate to severe post-thrombotic syndrome (PTS) in patients with acute iliofemoral deep vein thrombosis (IFDVT). However the impact of concomitant thrombus extension down to the popliteal veins on clinical and duplex sonographic outcomes is unknown.

**Methods:** In this post-hoc analysis of the pooled data from the randomized controlled BERNUTIFUL trial, which was investigating standard catheter-directed thrombolysis (CDT) versus ultrasound-assisted CDT in patients with acute IFDVT, we compared relevant clinical outcomes (incidence and severity of PTS assessed by the Villalta score and the revised venous clinical severity scores, rVCSS), disease-specific quality of live (QOL, CIVIQ-20 survey), and duplex sonographic outcomes at 12 months follow-up between patients with and without thrombus extension to the popliteal veins.

**Results:** Overall, 48 patients were included (48% of men, median age of 50 years), of whom 31 (65%) had IFDVT without and 17 (35%) with popliteal thrombus extension. Patients with popliteal DVT were older, had a higher body mass index and more important leg swelling. At 12 months, three (6.3%) patients died and 40 (88.9%) were free of PTS. Disease-specific QOL improved significantly from baseline to 12 months (50.6 +/- 14.5 vs. 27.9 +/- 10.2, P<0.01). There was no difference between the two groups regarding mortality (P=0.28), PTS assessed by total Villalta (P=0.67) and rVCSS scores (P=0.47), and disease-specific QOL improvement (P=0.14). All duplex sonographic outcomes were also similar between the two groups, except for more frequent post-thrombotic popliteal vein lesions and reflux (P=0.02 for both) in patients with popliteal involvement.

**Conclusion:** The one-year incidence and severity of PTS was very low among patients with acute IFDVT who underwent CDT, regardless of the presence or absence of initial popliteal DVT. However, post-thrombotic popliteal vein lesions and reflux are more frequent in IFDVT patients with popliteal involvement. Their impact on long-term outcomes remains to be investigated.

**Table I.** Baseline characteristics of patients with 12-months follow-up data

| | Total (n = 48) | Without popliteal DVT (n = 31) | With popliteal DVT (n = 17) | *P* value |
|---|---|---|---|---|
| **Demographics** | | | | |
| Age (years) | 50 ± 21 | 45 ± 22 | 59 ± 15 | 0,020 |
| Women | 25 (52) | 19 (61) | 6 (35) | 0,090 |
| Body mass index (kg/m2) | 27,3 ± 5,0 | 25,8 ± 4,0 | 30,5 ± 5,7 | 0,010 |
| Visual analogic pain scale | 3,2 ± 3,0 | 2,8 ± 2,9 | 3,7 ± 3,2 | 0,350 |
| **Risk factors and comorbidities** | | | | |
| Immobilisation* (< 3 mo) | 25 (52) | 16 (52) | 9 (53) | 0,930 |
| Current smoking | 16 (33) | 11 (35) | 5 (29) | 0,555 |
| Obesity | 16 (33) | 6 (19) | 10 (59) | 0,006 |
| Arterial hypertension | 16 (33) | 9 (29) | 7 (41) | 0,393 |
| Recent hospitalisation (< 3 mo) | 15 (31) | 9 (29) | 6 (35) | 0,654 |
| Hormone therapy ** | 14 (29) | 10 (32) | 4 (24) | 0,525 |
| Varicose veins or previous surgery for varicose veins | 11 (23) | 8 (26) | 3 (18) | 0,520 |
| Known family history of VTE | 11 (23) | 9 (29) | 2 (12) | 0,173 |
| Known previous VTE | 9 (19) | 6 (19) | 3 (18) | 0,885 |
| - known previous ipsilateral lower extremity DVT | 7 (15) | 5 (16) | 2 (12) | 0,682 |
| Dyslipidemia | 7 (15) | 3 (10) | 4 (24) | 0,229 |
| Chronic pulmonary disease | 6 (13) | 4 (13) | 2 (12) | 0,909 |
| Severe infection or sepsis (< 3 mo) | 6 (13) | 4 (13) | 2 (12) | 0,910 |
| Active cancer or treatment (< 6 mo) | 6 (13) | 3 (10) | 3 (18) | 0,425 |
| Peripheral artery disease | 5 (10) | 2 (6) | 3 (18) | 0,225 |
| Recent trauma (< 4 weeks) | 3 (6) | 3 (10) | 0 (0) | 0,185 |
| Coronary artery disease | 3 (6) | 1 (3) | 2 (12) | 0,242 |
| Diabetes | 3 (6) | 2 (6) | 1 (6) | 0,938 |
| Recent surgery (< 4 weeks) | 2 (4) | 2 (6) | 0 (0) | 0,285 |
| **Leg circumference difference index vs control leg (cm)** | | | | |
| Smallest ankle (B-measure) | 2,1 ± 1,5 | 1,5 ± 1,0 | 3,1 ± 1,7 | 0,003 |
| Largest calf (C-measure) | 4,5 ± 2,2 | 3,6 ± 1,6 | 6,3 ± 2,3 | 0,000 |
| Mid-thigh (F-measure) | 7,0 ± 4,3 | 5,9 ± 4,5 | 9,1 ± 3,1 | 0,037 |
| **Symptoms** | | | | |
| Leg swelling | 47 (98) | 30 (97) | 17 (100) | 0,454 |
| Leg pain | 43 (90) | 28 (90) | 15 (88) | 0,821 |
| Groin pain | 23 (48) | 18 (58) | 5 (29) | 0,057 |
| Back pain | 11 (23) | 9 (29) | 2 (12) | 0,173 |
| Leg redness | 17 (35) | 12 (39) | 5 (29) | 0,519 |
| **Time between symptom begin and catheter intervention** | | | | |
| Mean time (days) | 4,8 ± 3,7 | 5,2 ± 3,9 | 4,1 ± 3,4 | 0,313 |
| 1 to 3 days | 24 (50) | 15 (48) | 9 (53) | 0,763 |
| 4 to 7 days | 14 (29) | 9 (29) | 5 (29) | 0,978 |
| 8 to 14 days | 10 (21) | 7 (23) | 3 (18) | 0,687 |
| **Affected leg** | | | | |
| Left leg DVT | 33 (69) | 22 (71) | 11 (65) | 0,650 |
| Right leg DVT | 12 (25) | 7 (23) | 5 (29) | 0,600 |
| Bilateral DVT | 3 (6) | 2 (6) | 1 (6) | 0,940 |
| **Thrombus, involved vein segments** | | | | |
| Inferior vena cava | 8 (17) | 7 (23) | 1 (6) | 0,138 |
| Common iliac vein | 35 (73) | 24 (77) | 11 (65) | 0,343 |
| External iliac vein | 45 (94) | 30 (97) | 15 (88) | 0,242 |
| Common femoral vein | 45 (94) | 17 (90) | 28 (100) | 0,185 |
| Femoral vein | 38 (79) | 21 (68) | 17 (100) | 0,008 |
| Popliteal vein | 17 (35) | 0 (0) | 17 (100) | - |

*Note:* data presented as mean ± SD or number (%). * defined as bed ridden for > 72h, plaster cast, or long-distance travel of > 6h; **oral contraceptive pill, hormone replacement therapy or Tamoxifen use; DVT, deep vein thrombosis; VTE, venous thromboembolism

**Table II.** Interventional details and anticoagulation therapy of patients with follow-up data at 12 months

| | Total (n = 48) | Without popliteal DVT (n = 31) | With popliteal DVT (n = 17) | *P* value |
|---|---|---|---|---|
| **Catheter thrombolysis details** | | | | |
| mean total rTPa dose (mg) | 20,2 ± 1,4 | 20,3 ± 1,8 | 20,0 ± 0,0 | 0,460 |
| Mean treatment zone length (cm) | 42,7 ± 9,9 | 40,3 ± 10,9 | 47,1 ± 5,9 | 0,002 |
| Mean r-tPA dose per treatment zone centimeter (mg/cm) | 0,52 ± 0,21 | 0,56 ± 0,25 | 0,43 ± 0,07 | 0,044 |
| **Venous access site** | | | | |
| Inguinal | 2 (96) | 2 (6) | 0 (0) | |
| Popliteal | 46 (4) | 29 (94) | 17 (100) | |
| **Adjunctive interventional therapies** | | | | |
| Adjunctive catheter-based thrombus removal therapy | 18 (38) | 13 (42) | 5 (29) | 0,391 |
| - Rheolytic thrombectomy | 14 (29) | 10 (32) | 4 (24) | 0,525 |
| - Prolonged USAT | 6 (13) | 4 (13) | 2 (12) | 0,909 |
| Angioplasty and Venous stenting* | 39 (81) | 27 (87) | 12 (71) | 0,161 |
| - Mean number of stents | 1,4 ± 1,0 | 1,5 ± 1,0 | 1,0 ± 0,6 | 0,069 |
| - Stenting of inferior vena cava | 1 (2) | 1 (3) | 0 (0) | - |
| - Stenting of common iliac vein | 32 (67) | 24 (77) | 8 (47) | 0,033 |
| - Stenting of external iliac vein | 29 (60) | 21 (68) | 8 (47) | 0,161 |
| - Stenting of common femoral vein | 16 (33) | 10 (32) | 6 (35) | 0,831 |
| - Stenting of femoral vein | 3 (6) | 1 (3) | 2 (12) | 0,242 |
| **Anticoagulation, main type for first 3 months** | | | | |
| Vitamin K antagonist | 11 (23) | 9 (29) | 2 (12) | 0,388 |
| LMWH | 8 (17) | 5 (16) | 3 (18) | |
| Rivaroxaban | 29 (60) | 17 (55) | 12 (71) | |
| **Anticoagulation, duration** | | | | |
| Limited duration | 23 (48) | 17 (55) | 6 (35) | 0,180 |
| - 3 months | 12 (25) | 10 (32) | 2 (12) | |
| - 6 months | 6 (13) | 5 (16) | 1 (6) | |
| - 12 months | 5 (10) | 2 (6) | 3 (18) | |
| Extended duration | 25 (52) | 14 (45) | 11 (65) | |

*Note:* data presented as mean ± SD or number (%). *Angioplasty without stenting was not performed. CDT, catheter-directed thrombolysis; LMWH, low molecular weight heparin; r-tPA, recombinant tissue plasminogen activator; USAT, ultrasound-assisted catheter-directed thrombolysis

**Table III.** Clinical follow-up at 12 months

| | Total (n = 45) | Without popliteal DVT (n = 30) | With popliteal DVT (n = 15) | *P* value |
|---|---|---|---|---|
| **Villalta PTS scale** | | | | |
| Mean score | 2,0 ± 2,4 | 2,1 ± 2,2 | 1,8 ± 2,8 | 0,665 |
| No PTS (0-4 points) | 40 (89) | 26 (87) | 14 (93) | 0,168 |
| Mild PTS (5-9 points) | 4 (9) | 4 (13) | 0 (0) | |
| Moderate PTS (10-14 points) | 1 (2) | 0 (0) | 1 (7) | |
| Severe PTS (≥ 15 points or venous ulcer) | 0 (0) | 0 (0) | 0 (0) | |
| **Revised Venous Clinical Severity Score** | | | | |
| Mean total score | 2,7 ± 2,9 | 2,5 ± 2,7 | 3,1 ± 3,3 | 0,472 |
| Use of compression stockings | 1,2 ± 1,3 | 1,0 ± 1,2 | 1,5 ± 1,4 | 0,211 |
| - not used (0 points) | 20 (44) | 15 (50) | 5 (33) | 0,233 |
| - intermittent use of stockings (1 point) | 7 (16) | 4 (13) | 3 (20) | |
| - wear stockings most days (2 points) | 7 (16) | 6 (20) | 1 (7) | |
| - full compliance (3 points) | 11 (24) | 5 (17) | 6 (40) | 0,140 |
| **CEAP classification for CVD** | | | | |
| $C_0$ (No visible or palpable signs of venous disease) | 21 (47) | 15 (50) | 6 (40) | 0,451 |
| $C_1$ (Telangiectasies or reticular veins) | 13 (29) | 7 (23) | 6 (40) | |
| $C_2$ (Varicose veins only) | 6 (13) | 4 (13) | 2 (13) | |
| $C_3$ (Edema with or without varicose veins) | 0 (0) | 0 (0) | 0 (0) | |
| $C_4$ (Changes in skin and subcutaneous tissue secondary to CVD) | 4 (9) | 4 (13) | 0 (0) | |
| $C_5$ (Healed venous ulcer) | 1 (2) | 0 (0) | 1 (7) | |
| $C_6$ (Active venous ulcer) | 0 (0) | 0 (0) | 0 (0) | |
| **CIVIQ-20** | | | | |
| Baseline score (at 1 mo) | 52,1 ± 15,7 | 50,6 ± 14,5 | 54,8 ± 18,0 | 0,451 |
| End score (at 12 mo) | 27,9 ± 10,2* | 26,1 ± 6,2* | 31,1 ± 15,0* | 0,138 |

*Note:* data presented as mean ± SD or number (%). *$P$ < 0.01 vs. baseline CIVIQ-20 score. CEAP, Clinical Etiological Anatomical Pathophysiological; CVD, chronic venous disease; PTS, post-thrombotic syndrome; CIVIQ, Chronic Venous Insufficiency Questionnaire

**Table IV.** Duplex ultrasound studies at 12 month follow-up

| | Total (n = 45) | Without popliteal DVT (n = 30) | With popliteal DVT (n = 15) | *P* value |
|---|---|---|---|---|
| **Patency*** | | | | |
| Common iliac vein | 42 (100) | 30 (100) | 12 (100) | >0,99 |
| External iliac vein | 44 (98) | 29 (97) | 15 (100) | >0,99 |
| Common femoral vein | 44 (98) | 29 (97) | 15 (100) | >0,99 |
| Femoral vein | 40 (89) | 27 (90) | 13 (87) | >0,99 |
| Popliteal vein | 45 (100) | 30 (100) | 15 (100) | >0,99 |
| **Post-thrombotic lesions**** | | | | |
| Common femoral vein | 5 (11) | 4 (13) | 1 (7) | 0,651 |
| Femoral vein | 15 (33) | 7 (23) | 8 (53) | 0,091 |
| Popliteal vein | 13 (29) | 5 (17) | 8 (53) | 0,016 |
| Calf veins | 7 (19) | 3 (11) | 4 (44) | 0,045 |
| **Venous flow with respiratory variation** | | | | |
| Common iliac vein | 42 (100) | 28 (100) | 14 (100) | - |
| External iliac vein | 43 (98) | 29 (97) | 14 (100) | >0,99 |
| Common femoral vein | 44 (98) | 29 (97) | 15 (100) | >0,99 |
| Femoral vein | 39 (87) | 26 (87) | 13 (87) | >0,99 |
| **Reflux of > 1 second duration** | | | | |
| Common femoral vein | 9 (20) | 5 (56) | 4 (44) | 0,464 |
| Femoral vein | 11 (25) | 6 (21) | 5 (33) | 0,468 |
| Popliteal vein | 10 (23) | 3 (10) | 7 (47) | 0,019 |
| Calf veins | 1 (2) | 0 (0) | 1 (6) | 0,340 |

Note: Data presented as absolute numbers and (%), percentages may vary due to missing data. * defined as spontaneous orthograde venous flow; ** defined as webs, wall thickening, synechia etc

**FM 2.3**

## HIT antibody generation in major orthopedic surgery without heparin exposure

*M. Liebig[1], H. Kroll[2], E. Lindhoff-Last[1], I. Baumgartner[3], M. Schindewolf[3] ([1]Frankfurt DE, [2]Dessau DE, [3]Bern)*

**Objective:** Immune heparin-induced thrombocytopenia (HIT) is a life-threatening prothrombotic complication of heparin therapy caused by pathogenic anti-platelet factor 4 (PF4)/heparin antibodies. Orthopedic and cardiac surgery patients are at a higher risk of seroconversion (20–50%) compared to medical patients (<1%) without developing HIT sequelae like thrombocytopenia and arterial and venous thromboembolic complications. The reason for this observation is unclear. It is known that non-heparin glycosaminoglycans and sulfated polysaccharides may induce the antigenic epitope on PF4 relevant for sensitization. We hypothesized that glycosaminoglycans, i.e. chondroitin sulfates, released from articular cartilage during major orthopedic surgery might explain the high seroconversion rates.

The aim of our study was to determine the incidence of HIT antibodies in orthopedic surgery patients in the absence of heparin exposure when the direct oral factor Xa inhibitor rivaroxaban is used postoperatively for thrombosis prophylaxis instead of low-molecular weight heparin.

**Methods:** Laboratory HIT diagnostics were performed before and ≥5 days after surgery utilizing an immunogenic chemiluminescence test (HemosIL® AcuStar HIT-IgG(PF4-H)) and a functional heparin-induced platelet activation assay (HIPA). Exclusion criteria: Any heparin exposure within the previous 3 months as well as during and after surgery.

**Results:** 107 consecutive patients, 65 (60,7%) female, 42 (39,3%) male patients underwent 66 (61,6%) and 41 (38,3%) total hip and knee replacement surgeries, respectively. No seroconversion with generation of anti-PF4/heparin antibodies was observed in any of the study patients in both, the immunogenic and the functional assay, neither before or after surgery.

**Conclusion:** Major orthopedic surgery itself does not seem to be sufficient to trigger sensitization alone in the absence of heparin and, thus, does not seem to explain the high seroconversion rates observed in orthopedic surgery patients. Heparin seems to be indispensable for sensitization. However, further risk factors for triggering anti-PF4/heparin antibody formation, i.e. bacterial infections, extent of trauma, release of nucleic acids, may play a role. Because the antigenic complex is only induced at an optimal molar ratio of PF4 and heparin/glycosaminoglycan, it is conceivable that at least some of these factors need to concur to cause sensitization.

**FM 3.1**

## Catheter-directed thrombolysis for postpartum deep venous thrombosis

*M. Girona[1], C. Kohler[1], C. Säly[2], I. Baumgartner[1], M. Schindewolf[3] ([1]Bern, [2]Feldkirch AT)*

**Objective:** Venous thromboembolism is a major concern during pregnancy as well as in the postpartum period. In acute proximal deep venous thrombosis, endovascular recanalization with locally administered thrombolytic agents has evolved as therapeutic alternative to anticoagulation alone. However, data on the bleeding risk of thrombolysis in the postpartum period is limited.

**Methods:** We performed a review of the literature on CDT in the postpartum period, applying the following search terms in the pubmed database: ([peripartum OR postpartum OR pregnancy] AND thrombolysis), without any further search limits. In total, we found twenty six reports on single patients or small patient series including up to six women who had received CDT in the postpartum period.

**Results:** In total, twenty six reports on single patients or small patient series including up to six women who had received CDT in the postpartum period. No larger patient series and no randomized controlled trials were available. Twenty two procedures were described as successful and three procedures were described as partially successful (in six patients the result of the procedure was not specified). None of the reported patients developed major or life-threatening bleeding complications. In more than half of our reviewed patients, no information on PTS was given. Nevertheless, in the remaining fif-

teen patients, fourteen did not develope PTS, subsequently, and one showed only signs of mild PTS in the further course.

**Conclusion:** Major bleeding complications during CDT started > 2 days postpartum seem to be rare. However, larger case series or randomized controlled trials are needed to substantiate the findings.

## P 1

## Catheter-directed thrombolysis for the treatment of pulmonary embolism: Experience at a University Hospital.

*S. Zbinden, D. Voci, P. Kaufmann, N. Kucher, S. Barco (Zürich)*

**Objective:** Systemic thrombolysis for acute hemodynamically stable intermediate-risk pulmonary embolism (PE) reduced early decompensation and death, but was associated with an unacceptable rate of major and intracranial bleedings. Catheter-directed (ultrasound-assisted) thrombolysis (EKOS-lysis) is potentially effective to reverse right ventricular dysfunction without increasing the risk of bleeding.

**Methods:** We studied the course of hemodynamic improvement in consecutive acute PE patients treated at a University Hospital, 2018–2020. Patients with intermediate-high or high-risk acute PE were included and underwent EKOS-lysis with a standard regimen of 10 mg alteplase/catheter over 15 hours. Early and late clinical and hemodynamic outcomes were studied: (i) mean pulmonary arterial pressure (mPAP) before and after treatment; (ii) early death, hemodynamic decompensation within 7 and 30 days of treatment; (iii) early major and minor bleeding complications (ISTH definition) or device-related complications within 7 days of treatment.

**Results:** A total of 149 patients were identified. Data collection was completed for 142 patients. 86 patients (60.6%) were men and the mean age was 61.4 (SD 15.6) years. All patients received anti-Xa activity-adjusted unfractionated heparin. mPAP decreased from a mean of 35.5 (SD 8.9) to 25.8 (SD 6.9) mmHg (absolute difference 10 mmHg; 95%CI 6.6–13.5). One (0.7%) patient died and two (1.4%) hemodynamic decompensations were recorded within 30 days of hospitalization. One nonfatal major bleeding (0.7%) and three minor bleedings (2.1%) were observed. Two device-related complications were recorded.

**Conclusion:** Catheter-directed ultrasound-assisted thrombolysis rapidly reduced the mean pulmonary arterial pressure in intermediate-high or high-risk acute PE with an acceptable rate of major bleeding events.

**Table I.** Baseline characteristics

| | |
|---|---|
| **Demographics** | |
| Men, n/N (%) | 86/142 (60.6) |
| Age (years), mean (SD) | 61.4 (15.6) |
| **Clinical presentation** | |
| CPR, n/N (%) | 4/140 (2.9) |
| Sys Blood Pressure <90*, n/N (%) | 19/139 (13.7) |
| Catecholamine Therapy**, n/N (%) | 15/139 (10.8) |
| ICU pre-intervention, n/N (%) | 18/140 (12.9) |

*Notes.* CRP: Cardiopulmonary Resuscitation, ICU: Intensive care unit
*for >15 minutes
**necessary before CDT

**Table II.** Invasive Hemodynamic Measurements

| | Baseline (B) | Post-intervention (PI) |
|---|---|---|
| Pulmonary artery systolic pressure, mmHg, mean (SD) | 50.6 (13.1) | 35.4 (10.0) |
| Pulmonary artery diastolic pressure, mmHg | 27.1 (8.7) | 19.6 (6.4) |
| Pulmonary artery mean pressure, mmHg | 35.5 (8.9) | 25.8 (6.9) |

**Table III.** Outcomes

| | |
|---|---|
| Hemodynamic decompensation (7–30 days of treatment), n (%) | 2/140 (1.4) |
| Death (7–30 days of treatment), n (%) | 1/141 (0.7) |
| Recurrence of PE (30 days), n (%) | 4/138 (2.9) |
| Bleeding (30 days), n (%) | 4/141 (2.8) |
| Major Bleeding, n (%) | 1/141 (0.7) |
| Minor Bleeding, n (%) | 3/141 (2.1) |
| Stroke (30 days), n (%) | 1/142 (0.7) |
| Ruptures/malfunction/catheter related AEs (30 days), n (%) | 2/141 (1.4) |

## P 9

## Systemic Sclerosis of the leg arteries

*D. Herzog[1], R. Hügli[1], C. Von Arx[1], N. Willi[2] ([1]Bruderholz, [2]Liestal)*

**Objective:** We present a female patient with a manifestation of Systemic Sclerosis in her leg arteries.

**Methods:** The 71 year – old female patient complained about pain in the right calf after a walking distance of 150 Meters. Within 4 weeks she developed an ulcer of the forth toe of the right foot. The patient had no cardiovascular risk factors (non-smoker, no diabetes, no hypertension). She suffered from a Systemic Sclerosis, with recurrent esophageal stenosis. She was put on tadalafil (PDE – 5- inhibitor) as treatment of the Systemic Sclerosis 6 months before admission.

**Results:** The cinical investigation at the first ambulatory screening revealed a reduced macroperfusion of the right lower leg. The ancle – brachial– index (ABI) was reduced on the right side at rest (0.77) with significant reduction after performing 30 squats (0.35), on the left side the ABI was normal. Analysing the pulse wave curves we found pathological patterns at the foot level on both sides. New ulcers developed (third and fifth toe right side), followed by necrosis in the lesions within four weeks.

Performing another vascular ultrasound in follow up, we diagnosed a new occlusion of the right popliteal artery, pars 3, approximately 3 cm long.

Consequently, we performed percutaneous transluminal angioplasty (PTA) of the right popliteal artery in the first place, because of recurrent stenosis. a second PTA with Supera – Stent implantation in the right popliteal artery was performed. After the intervention, we saw a recanalized popliteal artery, again a normal ABI with then normal segmentoscillography curves. Unfortunately the further course was complicated in a way, that the patient developed osteomyelitis of the fourth and fifth toe of the right foot. The two toes had to be amputated 3 weeks after the first diagnosis of the lesions.

The amputation material was sent in for histologic analyses and we found, presumingly downstreamed embolization material in the small vessels of Dig V. Histologically there were also focal dermal sclerotic lesions and the small vessels showed intima proliferation without atheromas.

**Conclusion:** We present a case of female patient with an assumed lesion of a Systemic Sclerosis in the popliteal artery, and proven lesions in the small vessels of the amputated toes. Coincidently we found synthetic intravascular material, probably after repeated PTA and Stent implantation.

## P 11

### Major adverse limb events in patients with femoro-popliteal and below-the-knee peripheral arterial disease treated with either sirolimus-coated balloon or standard uncoated balloon angioplasty: The SirPAD randomized trial

*S. Barco, T. Sebastian, D. Voci, R. Spescha, N. Kucher (Zürich)*

**Objective:** Peripheral artery disease (PAD) is a progressive atherosclerotic disease with the majority of atherosclerotic lesions located in the femoro-popliteal arteries and less commonly in the infra-popliteal arteries. Drug-coated balloons (DCB) were developed to prevent neo-intimal proliferation and restenosis after PTA and a significant reduction in restenosis rates, late lumen loss, and incidence of target lesion re-vascularization was observed compared to the uncoated devices.
**Methods:** The investigator-initiated randomized controlled phase III SirPAD trial (NCT04238546) will show whether the use of sirolimus-coated balloon catheters is non-inferior to uncoated balloon catheters in infra-inguinal angioplasty to prevent one-year major adverse limb events (MALE), including unplanned major amputation of the target limb and target lesion re-vascularization for critical limb ischemia, in a representative population of patients with PAD (`all-comers`). If the criterion for non-inferiority is confirmed, the study will test whether sirolimus-coated catheters are superior to uncoated ones in the setting of predefined hierarchical superiority analyses. Assuming a 10% event rate (MALE) within 12 months of enrollment in both the control and intervention group, and a non-inferiority margin of 5% expressed as absolute risk difference, a total of 1132 patients (566 patients per treatment group) allow to show non-inferiority of the intervention group with a power of 80% and a type I error rate of alfa =2.5% one-sided.
**Results:** The rationale and design of the multicentre randomized controlled SirPAD trial as well as the status of enrolment and the general characteristics of recruited patients will be presented during the next USGG congress.

## P 12

### Enoxaparin for primary thromboprophylaxis in ambulatory patients with COVID-19: the multicentre randomized controlled investigator-initiated OVID trial. Study design, status or enrolment and patients overview

*S. Barco[1], D. Voci[1], R. Bingisser[2], G. Colucci[3], A. Frenk[4], B. Gerber[5], U. Held[1], F. Mach[6], M. Righini[6], T. Rosemann[1], T. Sebastian[1], R. Spescha[1], S. Stortecky[4], S. Windecker[4], P. Simioni[7], S. Konstantinides[8], D. Dürschmied[9], N. Kucher[1] ([1]Zürich, [2]Basel, [3]Lugano, [4]Bern, [5]Bellinzona, [6]Genf, [7]Padova IT, [8]Mainz DE, [9]Freiburg DE)*

**Objective:** Coronavirus disease (COVID-19) emerged as a public health crisis of global proportions characterized by a substantial risk of developing acute pulmonary embolism or deep vein thrombosis. It remains unclear whether ambulatory COVID-19 patients not admitted to the hospital may benefit from primary thromboprophylaxis.
**Methods:** The OVID study will show whether prophylactic-dose enoxaparin improves survival and reduces hospitalizations in symptomatic ambulatory patients aged 50 or older diagnosed with COVID-19. The primary efficacy outcome is a composite of any hospitalization or all-cause death occurring within 30 days of randomization. Enoxaparin (Clexane®) will be given at the recommended dose of 4,000 IU antiXa activity (40 mg/0.4 ml) once daily by SC injection for 14 days. The study is conducted as a multicentre randomized open-label controlled trial in Switzerland (6 centers), Germans (2 centers) and Italy (4 centers). The sample size calculation is based on the parameters alfa = 0.05 (2-sided), power = 1–beta = 0.8, event rate in experimental group, pexp = 0.09 and event rate in control group, pcon = 0.15. The resulting total sample size is 920 (plus drop-outs). The aim of the predefined interim analysis after 50% of the sample size is to decide on early termination for efficacy (superiority) or futility.
**Results:** The design of the multicentre randomized controlled OVID trial as well as the status of enrolment and the general characteristics of patients will be presented during the next USGG congress.

## P 13

### Behandlung von Ulkus Cruris Venosum (VLU) und diabetischem Fussulkus (DFU) mit intakter Fischhaut resultiert in kürzerer Zeit bis Wundverschluss im Vergleich zu „Standard of Care“

*T. Zehnder[1], H. Kjartansson[2] ([1]Thun, [2]Reykjavík IS)*

**Objective:** In der Schweiz existieren Richtlinien, dass Wunden, die vier Wochen nach adäquater Therapie (Standard of Care „SOC“) eine Flächenreduktion von weniger als 40–50% aufweisen, eine Behandlung mit Hautersatzprodukten angezeigt ist. Wir testeten einen neuartigen, ergebnisbasierten Behandlungsalgorithmus für Ulcus cruris venosum (VLU) und dem diabetischen Fußulkus (DFU), bei dem die Wunden nach Ablauf einer 4-wöchigen SOC-Phase entweder mit SOC oder intakter Fischhaut behandelt wurden.
**Methods:** Wir erstellten ein ergebnisbasiertes Prognosemodell unter Verwendung von Surrogatmarkern und Endpunkten der Wundheilung, um den Heilungsverlauf mit SOC-Behandlung zu prognostizieren. Wir konnten vorhersagen, ob VLUs und DFUs in Abhängigkeit der Wundflächenreduktion der ersten 4 Wochen bis Woche 20 bzw. 24 abheilen würden. 51 Fälle (26 VLUs und 25 DFUs) starteten die 4-wöchige SOC Phase. 21 Fälle wurden mit SOC weiterbehandelt, da die Wundflächenreduktion in der SOC-Phase >40–50% betrug, 21 Fälle mit Fischhaut, da die Wundflächenreduktion in der SOC-Phase <40–50% betrug und 9 Fälle wurden bereits während der SOC-Phase abgeschlossen.
**Results:** Die Wundfläche von 12 der mit Fischhaut behandelten Fälle reduzierte sich in der ersten 4 Wochen Behandlung >25% als mit SOC prognostiziert. 12 der mit Fischhaut behandelten Fälle waren im Zeit-

punkt der Publikation abgeheilt. 10 der 12 Wunden heilten >50 % früher ab als mit SOC prognostiziert. 5 der mit Fischhaut behandelten Fälle erreichten die prognostizierte Wundflächenreduktion nicht, bei 4 Fällen wurde die Behandlung mit Fischhaut abgebrochen (kein Zusammenhang mit Produkt).

**Conclusion:** Diese Pilotstudie zeigt, dass die Anwendung von Fischhaut bei behandlungsresistenten VLUs und DFUs zu einer schnelleren Wundheilung führt als mit SOC prognostiziert, während mit SOC behandelte Wunden meist den Modellvorhersagen folgten. Dieser Effekt war selbst bei Wunden beobachtbar, deren Wundfläche sich während der SOC-Phase vergrösserte.



# Phlebology

## FM 3.2

### Swiss Thermic Endovenous Catheter Therapy Registry (SWISSTECT Registry), safety and outcome study

*C. Lanz[1], C. Jeanneret-Gris[2] ([1]Basel, [2]Bruderholz)*

**Objective:** Endovenous thermic ablation (laser treatment or radiofrequency ablation) is a frequently used therapy of varicose veins. The aim of this study is to analyse its efficacy and safety with three follow-ups, focusing on the occlusion rate of the treated segments after one year and the occurrence of thrombotic complications within four weeks follow-up.

**Methods:** A total of 4'012 patients (n = 5'258 vein segments) with a treated varicose vein insufficiency of the trunk veins or tributaries of the great saphenous vein or the short saphenous vein were included in this multicentred descriptive study. The intervention, baseline data, vein insufficiency and medical history of the patient were collected prospectively and documented in the registry. We performed Duplex ultrasound examinations and clinical assessments on the follow-up visit one week, one month and one year after the intervention. The statistical analysis assessed the occlusion rate and the detected thrombotic complications.

**Results:** There were 4'993 vein segments with a follow-up after one week, 4'681 after one month and 2'703 vein segments after one year. The complication of a deep vein thrombosis occurred in 54 patients (0.7 % of the treated segment after one week, 0.7 % after one month). 3.6 % (n = 2) of the patients with the complication of a thrombosis, reported a positive family history of thrombotic events, whereas 16.4 % (n = 9) had a positive personal history for thrombosis. 90.9 % (n = 50) of the individuals with a thrombotic event received a thrombosis prophylaxis, 3.6 % (n = 2) did not receive any. Two pulmonary embolisms were detected at the follow-up visit after one week. The efficacy after one year was as follows: 96.8 % (n = 2'571) of the vein segments were still occluded, 2.3 % (n = 61) partially occluded and 0.9 % (n = 24) were open.

**Conclusion:** This study with a large study cohort shows a high efficacy of the endovenous thermic therapy of varicose veins in the setting of every day clinical work based on the large occlusion rate of the treated segment after one year. The occurrence of thrombotic complications within four weeks seems to be low, but should be assessed during the follow-up.

**Table I.** Participating centres and doctors of our study

| Name of the centre | Person in charge for the study | Location |
|---|---|---|
| | Prof. Dr. J. Hafner (Board member SGP) | |
| | PD Dr. D. Heim (Board member SGP) | |
| | Dr. R. Holzinger (Board member SGP) | |
| | Dr. P. Kern (Board member SGP) | |
| | Dr. S. Küpfer (Board member SGP) | |
| | Dr. J. Traber (Board member SGP) | |
| AL | Dr. A. Lauber | Luzern |
| BJ | Dr. J. Bamatter | Lausanne |
| BM | Dr. M. Bieli | Basel |
| BVZ | PD Dr. T. Willenberg | Bern |
| CHUV | Prof. Dr. L. Mazolai | Lausanne |
| CJ | Prof.Dr.C.Jeanneret-Gris(BoardmemberSGP) | Bruderholz |
| CP | PD Dr. P. Cassina (Board member SGP) | Lugano |
| DN | Dr. N. Ducrey (Board member SGP) | Lausanne |
| GAS | PD Dr. H. Uthoff | Luzern |
| GMA | PD Dr. H. Uthoff | Luzern |
| GPB | Dr. D. Müller | Biel |
| DE, ERP | Dr. D. Erni | Luzern |
| KSA | Dr. Gröchenig | Aarau |
| KSB | Dr. C. Rouden | Baden |
| KSO | Dr. B. Blum | Olten |
| LIM | Dr. T. Baldi | Zürich |
| RE | Dr. R. Eichlisberger | Arlesheim |
| SA | Dr. A. Steity | Lausanne |
| USB | Prof. Dr. D. Staub | Basel |
| VBK | Dr. D. Müller | Biel |
| VI | Dr. I von Planta | Basel |
| ZS | Dr. S. Zwicky | Thun |

## FM 3.3

### Thrombotic events after endovenous laser ablation with and without thromboprophylaxis: Insights from the VEINOVA Registry

*H.H. Keo[1,2], C. Regli[1], D. Staub[2], H. Uthoff[2,3] ([1]Aarau, [2]Basel, [3]Lucerne)*

**Objective:** Thrombotic events occur infrequently following saphenous vein laser ablation (EVLA). The aim of this retrospective study was to evaluate thrombotic events after EVLA with and without thromboprophylaxis.

**Methods:** Between October 2019 and June 2020 we retrospectively analyzed a consecutive series of patients undergoing endovenous laser ablation (EVLA) from the prospectively maintained VEINOVA Registry (VEIN Occlusion with VArious techniques) with and without postoperative thromboprophylaxis. EVLA was performed with a 1470 nm diode radial laser fiber. In the same session all insufficient tributaries were treated by phlebectomy or sclerotherapy. Tumescent local anesthesia with 1 % rapidocaine was applied perivenously. Laser treatment was carried out in a continuous mode with a power of 10 W aiming a LEED at 50–90 J/cm. Compression stockings were applied for one week. All patients were examined clinically and with duplex ultrasound prior to intervention, and at follow-up visits (1 week and 4 weeks) for occlusion rate and for EHIT class 2 or higher and VTE complications.

**Results:** A total of 249 patients were identified. 26 patients were omitted du to EVLA of recurrent varicose vein. 227 saphenous veins (159 GSV, 49 SSV, 19 AASV) in 225 legs of 223 consecutive patients were treated with EVLA and included in the final analysis. Mean age was 58.1 +– 13.8 years. Sixty (26.9 %) patients were male and 167 (73.1 %)

 

were female. CEAP C2 was found in 11 legs (4.5%), C3 in 123 (55.4%), C4a-c in 85 (58.3%) and C5–6 in 3 (1.4%). 91 (40.8%) patients did not receive thromboprophylaxis, 132 patients received thromboprophylaxis (in 98.5% rivaroxaban 10 mg OD and in 1.5% LMWH) for 3 days. Treatment length was 34.4 +– 19.3 cm. Mean diameter was 5.0 +– 1.3 mm. At one week follow no thrombotic event occurred in either group. At one month follow-up, 1 (1.1%) EHIT class 2 and 1 (1.1%) PE occurred in those without thromboprophylaxis and 1 (0.8%) VTE event occurred in those with thromboprophylaxis (p=0.36). Occlusion rate was 100% in both group at one week and at one month follow-up, respectively.
**Conclusion:** EVLA of incompetent saphenous veins using a 1470-nm diode laser appears to be safe with low thrombotic event rate with or without thromboprophylaxis. However, more data are need to draw a definitive conclusion.

## FM 3.4

### Safety, feasibility and early efficacy of a new 1940-nm diode laser: Insights from the VEINOVA Registry

*H. H. Keo[1], C. Somma[1], J. Lindenberg[2], D. Staub[3], N. Diehm[1], H. Uthoff[4] ([1]Aarau, [2]Baden, [3]Basel, [4]Lucerne)*

**Objective:** The aim of this study was to evaluate the safety, feasibility, and early efficacy of saphenous vein ablation with a newly-developed 1940-nm diode laser, which supposed to cause less pain and bruising using low linear endovenous energy density (LEED) .
**Methods:** Between July 2020 and June 2021 we retrospectively analyzed a series of patients undergoing endovenous laser ablation (EVLA) from the multi-center prospectively maintained VEINOVA Registry (VEIN Occlusion with VArious techniques). 173 saphenous veins (119 GSV, 29 SSV, 24 AASV, 1 PASV) in 152 legs of 136 consecutive patients were treated with EVLA.
EVLA was performed with a 1940 nm diode radial laser fiber. In the same session all insufficient tributaries were treated by phlebectomy or sclerotherapy. Tumescent local anesthesia with 1% rapidocaine was applied perivenously. Laser treatment was carried out in a continuous mode with a power of 3 W aiming a low LEED at 20–40 J/cm. Compression stockings were applied for one week. All patients were examined clinically and with duplex ultrasound prior to intervention, and at follow-up visits (2 days and 6 weeks) for occlusion rate and for EHIT and VTE complications.
**Results:** Mean age was 58.8 +– 15,4 years. Forty-four (32%) patients were male and 92 (68%) were female. Nearly half of the patients had a history of saphenous vein operation (47.8%). CEAP C2 was found in 23 legs (15.1%), C3 in 66 (43.4%), C4a-c in 57 (37.6%) and C5–6 in 6 (3.9%). Treatment length was 35.4 +– 18.3 cm. Mean diameter was 5.3 +– 1.2 mm. The average LEED was 36.6 +– 9.5 J/cm. The amount of the tumescent solution used was 125.5 1 +– 90.6 ml in total and 3.7 +– 2.4 ml /cm per treated saphenous vein. Concomitant miniphlebectomy was performed in 115 patients (84.6%). At 2 days and six weeks follow-up nearly all treated saphenous veins remained occluded (99.4%, and 99.4%, respectively). Only in 1 (0.7%) patient a partial recanalization occurred with no new reflux in the treated segments at 2 days and 6 weeks follow-up. No proximal DVT, PE or EHIT II-IV could be detected at follow-up. Only 1 (0.7%) patient had calf DVT at 6 weeks follow-up. Postoperative ecchymosis were rare (1.5%) and resolved at 6 weeks follow-up.
**Conclusion:** EVLA of incompetent saphenous veins using a new 1940-nm diode laser is feasible and appears to be safe and efficient with high occlusion rate needing minimal tumescent solution.

## FM 3.5

### Artificial Intelligence in the Research of Origins of Venous Insufficiency

*J. C. Ragg (Zürich)*

**Objective**: Artificial intelligence (A.I.) is currently increasingly used in research when large amounts of data have to be processed. According to definition, A.I. includes man-made „intelligent“ algorithms to simulate learning capabilities, different to simple data handling. In phlebology, to investigate the causes and progression of venous insufficiency, real longitudinal studies would require at least 10–20 years. A simulated timeline by help of A.I. could contribute to a better understanding.
**Methods**: A database with 18,111 epifascial leg vein valve videos of HR ultrasound examinations (16 – 32 MHz), 2018–2020) was evaluated using a novel A.I. Software (VeinBrain GmbH, CH) to determine objective criteria for congenital or acquired valve lesions. Furthermore, an attempt was made to chronologically classify successive changes in valve morphology and valve function using a specific algorithm package (A.I.M. V343) in order to simulate the history of epifascial insufficiencies.
**Results:** The A.I.-supported image analysis confirmed the hypothesis of embryonic missing valves, incomplete leaflets and commissural leakage (e-lesions), pressure-induced valve decompensations (p-lesions) and stasis-related valve degenerations (s- Lesions) in the age group up to 18 years of age at a probability level > 90%. The individual origin and history of primary leg venous insufficiency could be determined in 95.4% of the cases at the age of 18 years and younger, in 82.6% in patients between ages of 21 and 40 years and in 74.1% in patients between ages of 41 and 60 years. In patients above 60 years of age, the history could only be clarified for 31.2% of the cases due to overlapping and secondary damaging effects.
**Conclusion:** The A.I. software used in this study effectively supported the identification of various etiological types of primary epifascial insufficiency and contributed to a first simulation of 2 – 6 decades of progress. The most probable causes and progression mechanisms of the disease could be isolated for the majority of patients up to the age of 60. Although A.I. seems to expand research capabilities in medicine enormously, it should be remembered that still human factors decide about aims, correctness and quality.

## FM 3.6

### Comparison of the standardized Valsalva manoeuvre vs. the cuff deflation method to measure venous reflux

*D. Berther[1], C. Jeanneret-Gris[2] ([1]Basel, [2]Bruderholz)*

**Objective:** Two standardized methods are available to test venous reflux of the proximal leg veins: the Valsalva manoeuvre (VM) and the cuff deflation method (CM). This study investigates, whether the two methods are comparable.

**Methods:** In this study we used the cuff deflation method (CM) according to van Bemmelen and the Valsalva manoeuvre (VM) described by Jeanneret et al. We included 72 patients with varicose veins (VV) and 106 patients with deep vein thrombosis (DVT). The proximal leg veins (the common femoral vein (CFV), the femoral vein (FV), the great saphenous vein (GSV) were examined. A survey was sent to the members of the Union of Vascular Societies (UVS) to assess which methods are used in the clinical practice.

**Results:** In the VV-group the reflux time (RT) in seconds (median and IQR) for the VM and CM respectively, amounted to: 1.9 (1.8) and 2.4 (3.7) for the CFV (p = 0.004) and1.2 (2.6) and 1.5 (2.6) for the FV (p = 0.15). The correlation coefficient (VM vs CM) for the RT in the VV group amounted to 0.44 (p < 0.0001) for the CFV and 0.4 for the FV (p = 0.0003). The sensitivity ("venous severity score" > 5 = gold standard) of the two tests in the VV group amounted to 87.5% for both methods, using the RT as a parameter, in the CFV (p = 0.4). The sensitivity for the FV amounted to 87.5% for the VM and 71.4% for the CM (p = 0.4).

In the DVT – group the RT in seconds (median and IQR) for the VM and CM respectively amounted to: 0.9 (1.6) and 0.5 (2.3) for the CFV (p = 0.8), 0.8 (2.5) and 0.9 (3.5) for the FV (p <= 0.0001), and 0.4 (0.6) and 0.4 (0.6) for the GSV (p = 0.09). The correlation coefficient (VM vs CM) for RT in the DVT group, amounted to 0.62 for the CFV (p < 0.0001) and 0.77 for the FV (p < 0.0001), as well as 0.6 for the GSV (p < 0.0001). The sensitivity ("clinical score for postthrombotic syndrome" > 5 = gold standard) of the two tests in the DVT group was amounted to 50.0% for the VM and 42.9% for the CM in the CFV (p = 0.5). The sensitivity if reflux was measured in the FV, amounted to 42.9% for the VM and 50.0% for the CM (p = 0.5).

**Conclusion:** Both methods of reflux measurement (VM, CM) are comparable, detecting increased venous reflux and can be used side by side in clinical practice. The values for sensitivity measurements show, that both methods are better detecting venous insufficiency in varicose veins than in patients who suffered from deep vein thrombosis.

**P 2**

## Endovenous thermal ablation for treatment of symptomatic varicose veins- does weight matter?

*P. Boesch[1,2], E. Teruzzi[1,2], M. Hofer[1,2], D. Staub[2], H.H. Keo[3], H. Uthoff[1,2] ([1]Lucerne, [2]Basel, [3]Aarau)*

**Objective:** To study whether body weight affects the effectiveness and safety of endovenous thermal ablation for treatment of symptomatic varicose veins.

**Methods:** In this observational study the medical records of all patients who had ETA of the great saphenous vein (GSV), accessory saphenous vein (ASV), or small saphenous vein (SSV) between September 2017 and October 2020 were reviewed. All patients signed a written informed consent agreeing to use of their medical data anonymously for publication. Demographic data, vein characteristics, procedural data including concomitant phlebectomies and sclerotherapy and outcome data including ultrasound findings and complications were assessed.

**Results:** Between September 2017 and October 2020 in total 846 ETA interventions with 1241 treated truncal veins were performed in 679 patients. In 839 (99.2%) cases a concomitant phlebectomy with an average (±SD) treatment length of 69 ± 36 cm and in 182 (21.5%) cases a concomitant foam sclerotherapy was performed.

The mean±SD body-mass-index was 25.5±4.9 with a minimum BMI of 15.2 and a maximum BMI of 50.5. In 2.3% of the cases patients were underweight (BMI<18.5) and in 45.2% overweight (BMI >25) including 5.1% being obese with a BMI >35.

No significant association of weight with successful truncal vein ablation, minor or major bleeding, days of work loss, pain at day 1 and 7 after the intervention on visual analog scale, thrombotic events, infection, unplanned additional consultations or satisfaction with the intervention was observed.

**Conclusion:** This study shows that neither underweight nor overweight seem not to be associated with adverse outcomes such as infections or prolonged inability to work after ETA with phlebectomies. Given the minimal invasive nature of ETA, our results can reassure clinicians and patients that ETA varicose vein treatment is feasible and safe independent of the patients' weight.

**P 3**

## Endovenous thermal ablation for treatment of symptomatic varicose veins – occupational effects on procedure outcomes

*M. Hofer[1,2], P. Boesch[1,2], E. Teruzzi[1,2], D. Staub[2], H.H. Keo[2,3], H. Uthoff[1,2] ([1]Lucerne, [2]Basel, [3]Aarau)*

**Objective:** To study whether the occupational activity affects the effectiveness and safety of endovenous thermal ablation for treatment of symptomatic varicose veins.

**Methods:** In this observational study the medical records of all patients who had ETA of the great saphenous vein (GSV), accessory saphenous vein (ASV), or small saphenous vein (SSV) between September 2017 and October 2020 were reviewed. All patients signed a written informed consent agreeing to use of their medical data anonymously for publication. Demographic data, vein characteristics, procedural data including concomitant phlebectomies and sclerotherapy and outcome data including ultrasound findings and complications were assessed.

**Results:** Between September 2017 and October 2020 in total 846 ETA interventions with 1241 treated truncal veins were performed in 679 patients. In 839 (99.2%) cases a concomitant phlebectomy with an average (±SD) treatment length of 69±36 cm and in 182 (21.5%) cases a concomitant foam sclerotherapy was performed.

429 (55.6%) of the cases the patient were employed (E), in 64 (8.3%) self-employed (SE), in 42 (5.4%) unemployed (UE) and in 237(30.7%) retired (R). Profession data were missing in 74(8.7%) of the cases. 240 patients reported to work predominately (>80%) in the standing and 189 patients reported to work predominately in the sitting position.

The reported pain at day 1 was slightly lower in R than in the other groups (1.1±1.1 vs. 1.5±1.3, p<0.01) but no difference was observed at 7 days and 6 weeks after the intervention. The mean duration of analgesics intake was 2.7±2.4 days and did not differ between groups. However self-reported days of inability to work was significantly longer in E as compared to the other groups (3.9±2.6 (E), 2.8±1.9 (SE), 3.5±3.0 (UE) and 2.9±2.1 (R)). Patients with predominately standing position during work were significantly longer inca-

 

pable to work than patients with a predominantly sitting workplace (4.5±2.9 vs. 2.7±1.6 days, p<0.001).
No significant association with successful truncal vein ablation, bleeding, thrombotic events, infection or satisfaction with the intervention was observed.
**Conclusion:** Given the minimal invasive nature of ETA days of work loss are low. However, predominately working in the standing position is strongly associated with more days of work loss after ETA and employed patients were longer incapable to work than self-employed patients.

## P 4

## First experiences of combined proximal foam sclerotherapy and distal endovenous thermal laser ablation using an additional channel of a novel 6 French laser fiber for injection

*H. Uthoff[1,2], D. Staub[2], H.H. Keo[2,3] ([1]Lucerne, [2]Basel, [3]Aarau)*

**Objective:** Endovenous laser ablation (EVLA) has become the standard therapy for truncal vein insufficiency. In some circumstances, i.e. inguinal neovascularization after previous crossectomy without or only partial stripping of the truncal vein, additional foam sclerotherapy (ST) is necessary to treat (intrafascial) vein convolutes. However, due to early inactivation after contact with blood the foam effectiveness is decreased in larger veins especially if injected far away from the desired location of effect.
A novel 6 French laser fiber with an additional injection channel allows for distal injection with a proximal outlet for the sclerosant at the fiber tip. This allows for controlled intravascular proximal injection of a sclerosant even after administration of local tumescence analgesia and thus may represent a safer and more effective option to treat these patients completely.
The objective of the report our first experiences using this novel 6 French laser fiber with an additional channel for combined EVLA and proximal ST to treat symptomatic varicose veins.
**Methods:** The medical records of all patients with EVLA performed at a single centre between September 2020 and 2021 were reviewed. All interventions using the novel laser fiber with injection channel (Profiber, Biolitec) were identified and patients and procedure characteristics were obtained. Outcome parameters assessed at one day, one week and 6 weeks follow-up examinations were recorded.
**Results:** Between 09/2020 and 08/2021 eighteen combined EVLA/ST interventions in 16 patients with symptomatic, recurrent varicosis were performed (10 groin neovascularization and GSV, 6 popliteal neovascularisation and SSV, 2 tight perforator neovascularisation and GSV).
On average 4.5 [IQR3.25;4.5] ml of aethoxysklerol foam 3% (1:4 mixed with ambient air) was injected using the catheter, the mean diameter and length of the treated truncal vein was 6.2±3.2 mm and 23±4.1 cm. The reported post-procedural pain on the visual analog scale was in median 0.75 [IQR 0;1]. Duration of analgetics intake was 2 days [IQR 1.25;2.0]. No deep vein thrombosis or other clinically relevant complications were observed.

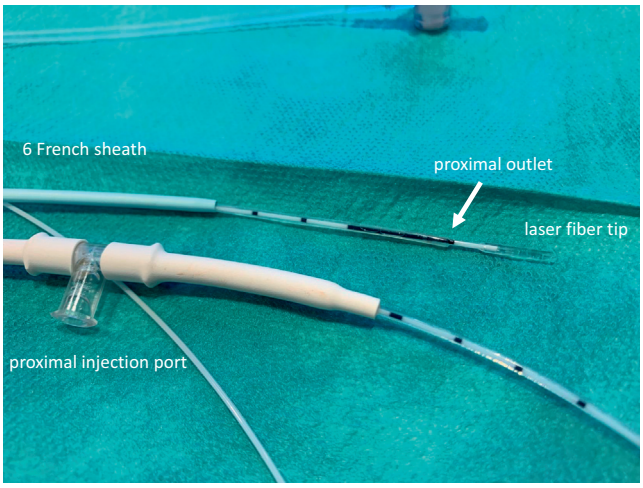


**Figure 1.** Detail view of the laser catheter with the injection port and distal outlet at the fibre tip.

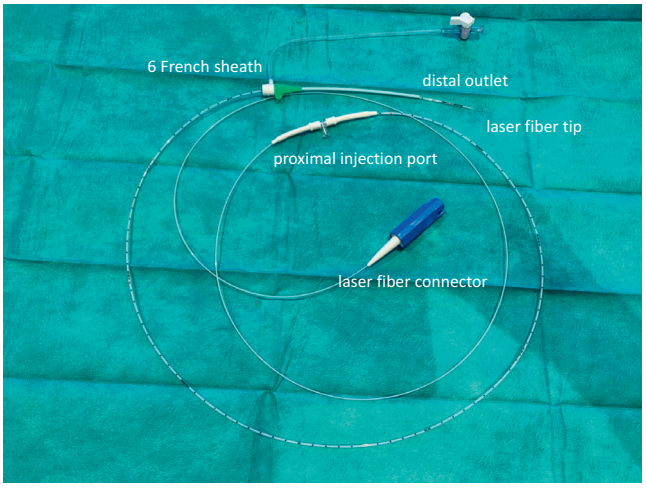


**Figure 2.** The novel 6 French laser fibre with an additional channel for proximal foam injection.

**Conclusion:** Early experiences indicate that the combined proximal foam sclerotherapy and distal endovenous thermal laser ablation using an additional channel of a novel 6 French laser fiber for injection seems to be safe and effective.

## P 7

## Endovenous thermal ablation for treatment of symptomatic varicose veins during summer time: hot or not

*E. Teruzzi[1,2], P. Boesch[1,2], M. Hofer[1,2], D. Staub[2], H.H. Keo[2,3], H. Uthoff[1,2] ([1]Lucerne, [2]Basel, [3]Aarau)*

**Objective:** To study whether endovenous thermal ablation performed during the hot summer season is safe or associated with a higher complication rate and/or impaired patients' comfort.

**Methods:** Medical records of all patients who had ETA of the great saphenous vein (GSV), accessory saphenous vein (ASV), or small saphenous vein (SSV) between September 2017 and October 2020 were reviewed. Demographic data, vein characteristics, procedural data including concomitant phlebectomies and sclerotherapy and outcome data including ultrasound findings and complications were assessed. For each intervention, the local peak outside temperature at the day and the 14 days after the intervention were collected using the data of the proximate meteorological station (IDAweb-MeteoSWISS). Days with a peak temperature >25 °C are defined as summer days, days with a peak temperature >30 °C are defined as very hot summer days.

**Results:** Between September 2017 and October 2020 in total 846 ETA interventions were performed.

In 839 (99.2%) cases a concomitant phlebectomy with an average (±SD) treatment length of 69±36 cm and in 182 (21.5%) cases a concomitant foam sclerotherapy was performed.

The mean peak temperature on the day of intervention was 14.0 °C (SD±8.2 °C) with a minimum and maximum temperature of –1 °C and 32.9 °C, respectively. In 109 (12.9%) of the cases the peak temperature was >25 °C and in 11 (1.3%) of the cases >30 °C.

The highest temperature recorded within the first 14 days after treatment was on average 19.0±7.2 °C with a minimum and maximum of –1 °C and 35.9 °C. In 261 (30.9%) of the cases the peak temperature was >25 °C and in 78 (8.4)% of the cases >30 °C.

No significant association of the peak temperature at the day of intervention as well as of the peak temperature within the first 14 days after intervention with succesful truncal vein ablation, minor or major bleeding, days of work loss, pain at day 1 and 7 after the intervention on visual analog scale, thrombotic events, infection, unplanned additional consultations or satisfaction with the intervention was observed.

**Conclusion:** Given the minimal invasive nature of ETA, our results can reassure clinicians and patients that ETA varicose vein treatment is possible and safe throughout the year, even on hot or very hot summer days. Thus, ETA procedures can also be performed in summer time.

## P 10

## Duration of post-sclerotherapy hyperpigmentation in patients with and without anticoagulation

*A. Münkhoff[1,2], R. Clemens[1], D. Staub[2], D. Hasselmann[1] ([1]Baden, [2]Basel)*

**Objective:** Appearance of hyperpigmentation after ultrasound guided foam sclerotherapy (UGFS) of varicose veins using aethoxysclerol is a common side effect. It is reported in 10–30% of cases persisting up to 18 months. This is affecting the overall satisfaction, even when aesthetics is not the indication. Hyperpigmentation is primarily caused by endothelial inflammation with extravasation of erythrocytes into the epidermis. Patients with risk of deep venous thrombosis after venous intervention, receive prophylactic anticoagulation postprocedural. We investigated whether administration of a prophylactic anticoagulation after UGFS may reduce the duration of hyperpigmentation.

**Methods:** Patients with varicose veins (CEAP classification of C2 and C3) treated at our institution between 2016 and 2018 who developed post-sclerotherapy hyperpigmentation were retrospectively included. A quality check questionnaire was sent two years after treatment to all patients treated at our institution. Patients were asked about the appearance of hyperpigmentation and the duration until it disappeared. Medical charts were reviewed whether prophylactic anticoagulation was received after treatment or not.

**Results:** Among 349 patients treated in our institution and 143 questionnaires returned, 57 patients (82% female) developed post-sclerotherapy hyperpigmentation on self-reporting and met the criteria to be included in this analysis. The median age was 59 years (interquartile range: 48–67 years). In total, 20 patients received any anticoagulation after the intervention and 37 patients did not. Using an ordinal logistic regression model, we found that for patients taking prophylactic anticoagulation, the adjusted odds of having hyperpigmentation lasting more than 6 months (versus less than or equal to 6 months) were 2.66 times higher (95% CI 0.83–9.07, p = 0.11) than for patients not taking anticoagulants.

**Conclusion:** We could show a trend toward longer hyperpigmentation but no significant difference between the patients with and without prophylactic anticoagulation after UGFS , while we first postulated, that the duration of hyperpigmentation may be reduced by it.

**Table I.** Base line characteristics

| Variable | level | Overall | No anticoagulation | Anticoagulation |
|---|---|---|---|---|
| n | | 57 | 37 | 20 |
| Age (median [IQR]) | | 59.00 [48.00, 67.00] | 58.00 [46.00, 67.00] | 61.00 [51.00, 67.25] |
| Gender | F | 47 (82.5) | 30 (81.1) | 17 (85.0) |
| | M | 10 (17.5) | 7 (18.9) | 3 (15.0) |
| Weight (median [IQR]) | | 69.00 [62.25, 78.25] | 67.00 [59.50, 73.50] | 72.00 [65.50, 80.00] |
| Treated_vein (%) | truncal vein | 3 (5.3) | 1 (2.7) | 2 (10.0) |
| | side branch | 24 (42.1) | 15 (40.5) | 9 (45.0) |
| | both | 30 (52.26) | 21 (56.8) | 9 (45.0) |
| Relapse (%) | no | 30 (52.26) | 18 (48.6) | 12 (60.0) |
| | yes | 27 (47.4) | 19 (51.4) | 8 (40.0) |
| Inzisision (%) | no | 44 (77.2) | 29 (78.4) | 15 (75.0) |
| | yes | 13 (22.8) | 8 (21.6) | 5 (25.0) |
| Polidocanol (%) | <=2 | 25 (44.6) | 19 (51.4) | 6 (31.6) |
| | >2 | 31 (55.4) | 18 (48.6) | 13 (68.4) |
| Duration_ | 1 | 4 (7.0) | 2 (5.4) | 2 (10.0) |
| Hyperpigmentation (%) | 2 to 3 | 7 (12.3) | 6 (16.2) | 1 (5.0) |
| | 4 to 6 | 11 (19.3) | 9 (24.3) | 2 (10.0) |
| | 7 to 11 | 14 (24.6) | 7 (18.9) | 7 (35.0) |
| | 12 to 17 | 7 (12.3) | 4 (10.8) | 3 (15.0) |
| | >18 | 14 (24.6) | 9 (24.3) | 5 (25.0) |

*Notes.* Only patients with hyperpigmentation are included. % latex table genereaded in R 4.0.2 by xtable 1.8-4 package % Tue Apr 13 11:01:01 2021

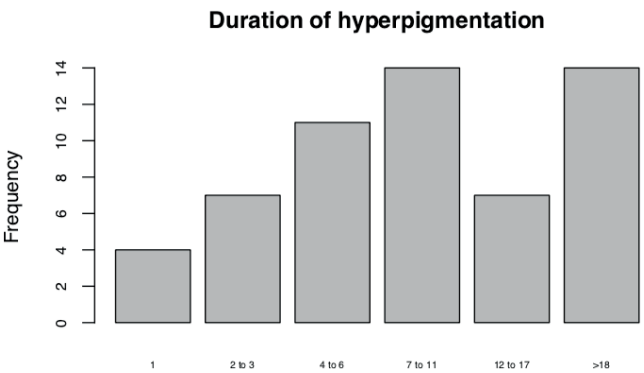


**Figure 1.** Duration of hyperpigmentation in all patients.

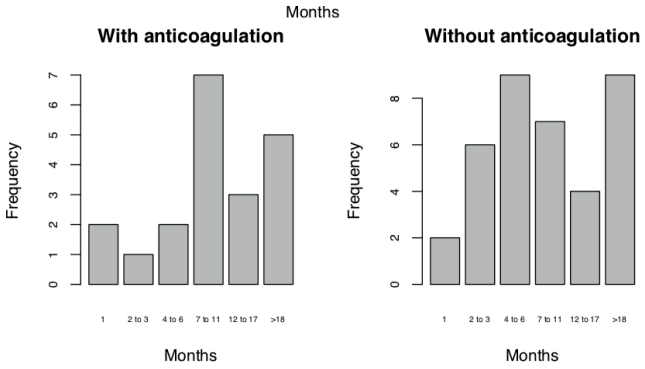


**Figure 2.** Duration of hyperpigmentation with and without anticoagulation.

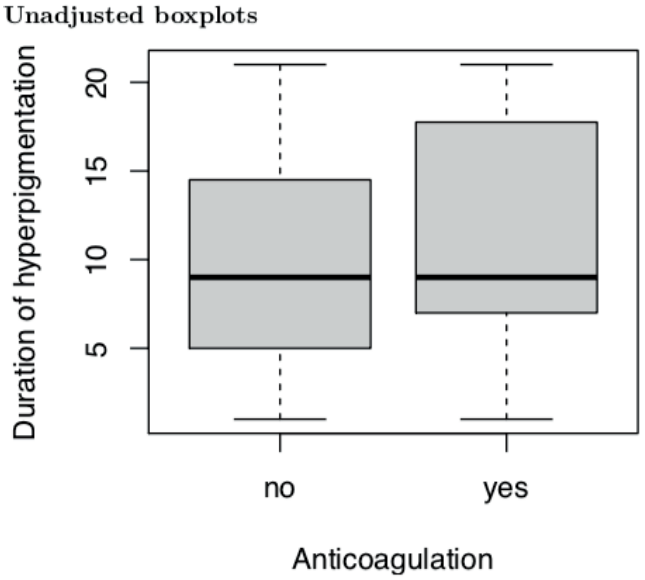


**Figure 3.** Sensitive analyze taking the middle point of each category as response.

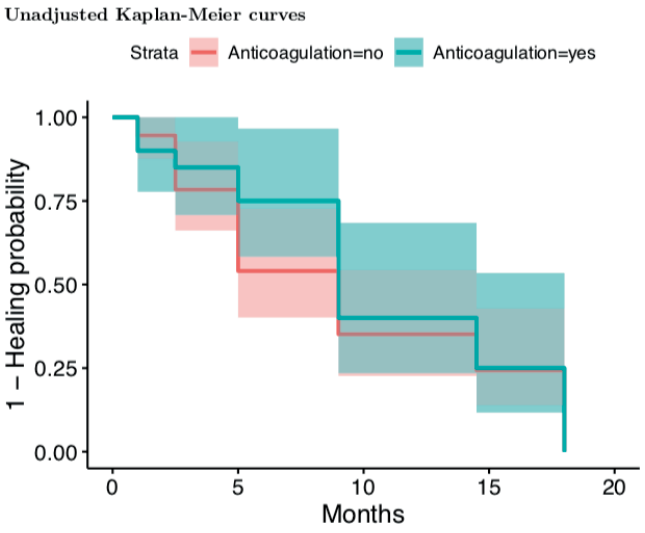


**Figure 4.** Taking the middle point of each category as response and considering observations in category >18 as censored.



# SSMVR

## FC 1.1

### Endothelial apelin signaling maintains progenitor cells to sustain intestinal tumor growth

*J. Bernier-Latmani[1], C. Cisarovsky[1], S. Mahfoud[1], S. Ragusa[1], I. Dupanloup[1], D. Barras[1], F. Renevey[1], S. Nassiri[1], P. Anderle[1], M.L. Squadrito[1], S. Siegert[1], S. Davanture[1], A. Gonzalez Loyola[1], N. Zangger[1], S. Luther[1], R. Benedito[2], P. Valet[3], B. Zhou[4], ([1]Lausanne, [2]Madrid ES, [3]Toulouse FR, [4]Shanghai CN)*

**Objective:** Stem and progenitor cells drive the majority of colorectal cancers (CRCs), yet vascular contribution to this niche remains largely unexplored. VEGFA is a key driver of physiological and tumor angiogenesis. Accordingly, current anti-angiogenic cancer therapies target the VEGFA pathway. However, many cancers are resistant to VEGFA blockade, but mechanisms driving this resistance remain unclear.
**Methods:** An array of genetic and orthotopic tumor models of CRC were tested with either VEGFA signaling blockade or apelin deficiency to assess the impact of these pathways for tumor growth. Mouse tissues and tumors were analyzed by 2D and 3D high resolution imaging and by gene expression analyses.
**Results:** Here we report that in CRC expansion of stem/progenitor pool requires VEGFA-independent growth and remodeling of blood vessels. Epithelial transformation induced expression of the endothelial peptide apelin, which directed migration of distant venous endothelial cells towards progenitor niche vessels ensuring optimal perfusion. In the absence of apelin loss of injury-inducible epithelial progenitors inhibited both incipient and advanced intestinal tumor growth.
**Conclusion:** Our results establish fundamental principles for the reciprocal communication between vasculature and the intestinal progenitor niche and provide a mechanism for resistance to VEGFA-targeting drugs in CRCs.

## FC 1.2

### T-cadherin is a novel regulator of pericyte function and interactions with endothelial cells during angiogenesis.

*M. Filippova, B. Dasen, S. Pigeot, G.M. Born, I. Martin (Basel)*

**Objective:** Pericytes play a key role in regulation of angiogenesis. Cadherins are adhesion molecules controlling morphogenesis and the maintenance of tissue architecture. Until recently N-cadherin remained the only cadherin described in pericytes. We have discovered that pericytes also express T-cadherin, an atypical GPI-anchored member of the superfamily. The aim of the study was to investigate T-cadherin function in pericytes and endothelial-pericyte interactions during angiogenesis.
**Methods:** T-cadherin expression in pericytes from different organs and tissues was analyzed by immunohistochemistry. Overexpression

or silencing of T-cadherin in human cultured pericytes was achieved using lentiviral vectors. The following assays were used to study T-cadherin effects in pericytes: proliferation, migration, invasion in fibrin gel, angiogenesis in Matrigel, angiogenesis in subcutaneous scaffolds in vivo. To analyze endothelial-pericyte interactions during sprouting angiogenesis we have developed a novel bioengineered multiwell slide-based in vitro model emulating the cellular composition and architecture of a microvessel.

**Results:** T-cadherin silencing inhibited pericyte proliferation, migration and invasion and resulted in the loss of pericyte ability to modulate endothelial angiogenic activity in vitro and in vivo. Overexpression, in contrast, promoted pericyte migration, invasion and interactions with endothelial cells during angiogenesis. Effects of T-cadherin on pericyte function were associated with changes in cell morphology, reorganization of the cytoskeleton, modulation of cyclin D1, αSMA, integrin β3, metalloprotease MMP1 and collagen expression levels, and involved Akt/GSK3β and ROCK intracellular signaling pathways.

**Conclusion:** Taken together, our data support that T-cadherin is required for pericyte proliferation and invasion, while T-cadherin loss shifts cells towards the myofibroblast state rendering them unable to control endothelial angiogenic behavior. The novel multiwell microchannel slide for analysis of sprouting angiogenesis is easy to handle, reproducible, can be "tailored" to include any components of interest and may represent a potential attractive standardized solution for studies on sprouting angiogenesis in vitro.

## FC 1.3

### Loss of HIF-1α in Natural Killer cells inhibits tumour growth by stimulating non-productive angiogenesis

*E. Krzywinska, M. Sobecki (Zürich)*

**Objective:** Productive angiogenesis, a prerequisite for tumour growth, depends on the balanced release of angiogenic and angiostatic factors by different cell types within hypoxic tumours. Natural Killer (NK) cells kill cancer cells and infiltrate hypoxic tumour areas. Cellular adaptation to low oxygen is mediated by Hypoxia-inducible factors (HIFs).

**Methods:** To test the role of the HIF pathway in NK cells during tumor growth, we generated mice with an in vivo, targeted deletion of HIF1-α specifically in NK cells via crosses of the loxP-flanked Hif1a allele to the Ncr1 (NKp46) promoter-driven Cre recombinase, resulting in Hif1αfl+/fl+/Ncr1cre+ mice, termed HIF1-α KO.

**Results:** We found that deletion of HIF-1α in NK cells inhibited tumour growth despite impaired tumour cell killing. Tumours developing in these conditions were characterized by a high density network of immature vessels, severe hemorrhage, increased hypoxia and facilitated metastasis due to non-productive angiogenesis. Loss of HIF-1α in NK cells increased the bioavailability of the major angiogenic cytokine Vascular Endothelial Growth Factor (VEGF) by decreasing the infiltration of NK cells that express angiostatic soluble VEGFR-1.

**Conclusion:** In summary, this identifies the hypoxic response in NK cells as an inhibitor of VEGF-driven angiogenesis, yet, this promotes tumour growth by allowing the formation of functionally improved vessels.

## FC 1.4

### Sodium Thiosulfate promotes angiogenesis via metabolic reprogramming of endothelial cells

*D. Macabrey, J. Joniová, A. Longchamp, G. Wagnière, J.-M. Corpataux, S. Deglise (Lausanne)*

**Objective:** Effective therapies to accelerate vascular repair are currently lacking. Pre-clinical studies suggest that hydrogen sulfide ($H_2S$), an endogenous gasotransmitter, promotes angiogenesis. Here, we hypothesized that sodium thiosulfate (STS), a clinically relevant source of thiol and potential $H_2S$ mimetic, stimulates angiogenesis and vascular repair.

**Methods:** Male C57BL/6J mice subjected to hindlimb ischemia were treated systemically with STS. Leg perfusion was measured by laser Doppler imaging and vascular density was assessed by immunofluorescence on frozen gastrocnemius muscles. The pro-angiogenic effect of STS was further assessed using a subcutaneous matrigel plug assay and a chick chorioallantoic membrane angiogenesis assay. Migration and proliferation of primary human umbilical endothelial cells (HUVEC) exposed to STS were measured using a wound healing assay and BrDU incorporation, respectively. HUVEC respiration and glycolysis were measured in a seahorse apparatus.

**Results:** STS stimulated arteriogenesis and vascular repair in mice following hindlimb ischemia as evidence by increased perfusion measured by laser Doppler imaging and by increased vascular density in the gastrocnemius muscle. STS also promoted angiogenesis in a matrigel plug assay and in the chick chorioallantoic membrane assay. In vitro, STS inhibited mitochondrial respiration and promoted glycolysis in HUVECs, which stimulated cell proliferation, migration and angiogenesis.

**Conclusion:** STS, a clinically relevant source of sulfur, promotes angiogenesis and revascularization in a mouse model of hindlimb ischemia. STS probably acts through metabolic reprogramming of endothelial cells towards a more proliferative glycolytic state. These findings may hold broad clinical implications for patients suffering from vascular occlusive diseases.

## FC 2.1

### 5' scRNA-seq reveals vessel subtype-specific transcriptional reprogramming in the chronic inflammatory skin disease psoriasis

*Y. He[1], J. Kim[1], J. Moody[2], C. Tacconi[3], E. Gousopoulos[1], F. Anzengruber[1], M. Julia-Tatjana[1], G. Restivo[1], L.C. Dieterich[1], M.P. Levesque[1], N. Lindenblatt[1], J.W. Shin[2], C.C. Hon[2], M. Detmar[1] ([1]Zürich, [2]Kanagawa JP, [3]Milan IT)*

**Objective:** Psoriasis is a chronic inflammatory skin disease characterized by epidermal thickening and hyperkeratosis, immune cell infiltration and vascular enlargement. Despite the emerging recognition of vascular normalization as a novel strategy in managing psoriasis, an in-depth delineation of the remodeled dermal vasculature has been missing.

**Methods:** In the present study, we exploited 5' single-cell RNA-sequencing (scRNA-seq) to investigate the transcriptomic alterations in

 

different subpopulations of blood vascular and lymphatic endothelial cells (ECs) directly isolated from psoriatic and normal human skin.
**Results:** Individual subtypes of ECs underwent specific molecular repatterning associated with cell adhesion and extracellular matrix organization. Blood capillaries, in particular, adopted post-capillary venule-like characteristics during chronic inflammation that are more permissive to trans-endothelial migration of leukocytes. We also identified psoriasis-specific interactions between cis-regulatory elements (CREs) for each EC subtype, revealing a transformed gene-regulatory network in psoriasis.
**Conclusion:** Together, these results identify specific transcriptional changes of ECs lining different vessel compartments upon chronic inflammatory conditions.

## FC 2.2

### Immune modulation of dendritic cells within afferent lymphatic vessels

*R. Montecchi, M. Hunter, J. Dang, I. Kritikos, C. Halin Winter, H. Tatliadim, V. Collado (Zürich)*

**Objective:** The transport of antigen and leukocytes from peripheral tissues via afferent lymphatics to draining lymph nodes (dLNs) is pivotal for the induction and regulation of adaptive immunity. Performing intravital microscopy (IVM) in inflamed murine ear skin, we recently reported that dendritic cells (DCs) and T cells that have entered into lymphatics spend several hours actively crawling and interacting with each other within skin lymphatic capillaries. Here, we set out to identify the T cell subset involved in intralymphatic DC-T cell interactions and to investigate their functional significance.
**Methods:** Performing FACS experiments we confirmed a previous study showing that regulatory T cells (Tregs) are a major fraction of T cells exiting from inflamed skin. IVM in triple-fluorescent reporter mice revealed that Tregs indeed enter into lymphatic capillaries and engage in interactions with DCs. Further analyses showed that intralymphatic interactions were more frequent compared to those occurring in the interstitial tissue. Considering that Tregs are well known to suppress the antigen-presenting functions of autoantigen presenting DCs by reducing levels of DC-expressed costimulatory molecules, we next performed in vivo adoptive transfers experiments.
**Results:** Upon co-transfer of WT and MHCII-/- DCs into inflamed skin we observed that MHCII-deficient DCs arriving in dLNs expressed higher CD80/CD86 levels in comparison to WT DCs. By contrast, adoptively transferred WT and MHCII-/- DCs remaining in inflamed skin expressed similar levels of CD80/CD86. Similarly, also treatment with MHCII-blocking antibodies increased the expression of CD80/CD86 in adoptively transferred DCs arriving in dLNs. We next plan to confirm the involvement of Tregs in the regulation of CD80/CD86 levels on migratory DCs, by performing adoptive transfers in Treg-depleted mice or in mice with monospecific Treg populations. In skin crawl-out assays, where DCs emigrate via lymphatics into the culture medium, we will study whether Treg-mediated suppression takes place during migration through afferent lymphatics – in contrast to occurring in dLNs.
**Conclusion:** Overall, our findings suggest that DC-Treg interactions within afferent lymphatics may help to modulate DC antigen-presenting functions. By suppressing CD80/CD86 levels in autoantigen presenting DCs, the latter could be important for the maintenance of tolerance.

## FC 2.3

### Elucidation of the relationship of cerebrospinal fluid flow pathways and the localization of myeloid cells during neuroinflammation

*L. Xin, D. Ivan, J. Steudler, A.A. Ganguin, G. Valentino, S. Aleandri, P. Luciani, G. Locatelli, S. Proulx (Bern)*

**Objective:** To investigate potential associations between the pathways of CSF flow and the localization of resident and blood-derived myeloid cells in autoimmune neuroinflammation.
**Methods:** We injected DiD fluorescently-labeled liposomes custom-designed for macrophage uptake to the lateral ventricle of CX3CR1-GFP//CCR2-RFP mice, a dual reporter mouse allowing visualization of CNS microglia/resident macrophages and blood-derived myeloid, respectively. Injections were made into either naïve mice or those that have been induced with experimental autoimmune encephalomyelitis (EAE), an animal model for multiple sclerosis. Two hours post intraventricular injection, mice were sacrificed, and the cranium and spinal column were decalcified for further analysis, including immunofluorescence staining and confocal imaging.
**Results:** Compared to naïve mice, we observed a limited liposome distribution to the lower spinal cord in EAE mice, while liposomes can be observed in both groups to be internalized by macrophages located in the cervical and upper thoracic spinal cord subarachnoid spaces. In the direction from cervical to sacral spine segments, there was an increasing number of CCR2+ infiltrates in the subarachnoid space and parenchyma, and a significantly reduced laminin expression on the surface of spinal cord. Along with these changes in spinal cord, we observed an enrichment of CCR2+ infiltrates along the drainage pathways where lymphatic vessels have been shown to absorb CSF, for example, above the cribriform plate, around the optic nerve and at the dura mater lining the dorsal skull. Moreover, there were clear increases of immune cells around the choroid plexus in all ventricles.
**Conclusion:** Our data suggest that CCR2+ myeloid cells follow the transport of CSF through the subarachnoid space during neuroinflammation. These infiltrating cells appear to traffic (or flow) to different anatomical locations, from where they breach encountered CNS barriers, such as superficial glia limitans of spinal cord. With increasing disease severity, CSF flow is reduced allowing exacerbation of the phenotype. To further test this hypothesis, we will perform in vivo near-infrared imaging of CSF flow at several disease stages. Our study provides insights into the pathological mechanisms autoimmune neuroinflammation and may lead to more effective therapies in the future.

## FC 2.4

### Targeted activation of lymphatic vessels enhances diabetic wound healing

*L.M. Brunner, N. Cousin, B. Schmucki, J. Scholl, L. Ducoli, S. Supersaxo, Y. He, M. Detmar (Zürich)*

**Objective:** Chronic wounds and the increasing prevalence of their risk factors, such as diabetes and vascular diseases, represent a major therapeutic challenge. The contribution of lymphangiogenesis, the growth and formation of lymphatic vessels, has remained largely



 

unexplored in wound healing. Lymphatic drainage and function seem to be impaired in chronic ulcers and lymphatic vessels can be absent in chronic wounds. We hypothesized that lymphatic vessels might play a role in wound healing and that targeted lymphatic activation might improve healing and quality of diabetic wounds.

**Methods:** Full-thickness excisional wound healing studies were conducted in wild-type (FVB), transgenic mice with an increased number of cutaneous lymphatic vessels (K14-VEGF-C) and transgenic mice which lack lymphatic vessels in the skin (K14-VEGFR3-Ig) mice. Macroscopic wound closure was monitored in vivo. Wounds and unwounded skin were harvested for histology and whole-wound RNA-bulk sequencing at different time points (3, 7 and 10 days). Db/db diabetic mice were treated either with a recombinant F8-VEGF-C fusion protein (targeting the VEGF-C protein to wounds via binding to the EDA fibronectin splice variant) or a control protein (SIP-F8) i.v. every other day and wounds were harvested 10 days post-wounding. Histology was performed for quantifications (H&E for morphology, Lyve1-CD31 co-stain for lymphatic vessels, a-SMA for myofibroblasts, Herovici stains for collagen maturation).

**Results:** The peak of lymphangiogenesis occurred at a rather late phase of wound healing from 7 to 14 days post-wounding. We observed that wounds closed more slowly in K14-VEGFR3-Ig mice and that these wounds showed an increased epidermal thickness 10 days post-wounding. K14-VEGF-C mice showed a reduced myofibroblast density 7 days post-wounding, while collagen maturation was delayed 14 days post-wounding. Diabetic mice treated with F8-VEGF-C showed a significant increase in lymphatic vessels 10 days post-wounding and their wounds closed faster than in control-treated animals.

**Conclusion:** Activation of lymphatic vessels with the F8-VEGF-C fusion protein accelerated diabetic wound healing, indicating a new strategy to treat diabetic wounds in the future.

## P 14

## Cerebrospinal fluid outflow via nasal lymphatics in mice: In detail investigation of lymphatic vessel structure and changes with age

*N. Cousin[1], M. Ries[1], A. Egger[1], J. Scholl[1], S. Proulx[2], M. Detmar[1]*
*([1]Zürich, [2]Bern)*

**Objective:** Previous studies have demonstrated a decline of lymphatic drainage of the cerebrospinal fluid (CSF) in aged mice and suggested that reduced drainage dynamics of waste products such as beta-amyloid peptides might contribute to Alzheimer's disease pathogenesis. In the present study, we aimed to characterize in detail the lymphatic vessels responsible for CSF drainage in mice and how they change with age.

**Methods:** Injection of dyes (tomato lectin, FITC-dextran) or/and conjugated antibodies (LYVE1-FITC, CD31-APC) into the CSF via the cisterna magna (CM) in Prox1-GFP or Prox1-TdTomato reporter mice was conducted. Mouse skulls began a decalcification protocol 50 minutes after injection and were then sectioned sagittally. Using immunofluorescence, the lymphatic vessels in the nasal submucosa were characterized by using markers such as LYVE1, Podoplanin, CD31, alpha-SMA and VE-Cadherin. Furthermore, lymphatic coverage at the site of the cribriform plate (CP) was quantified by immunofluorescence in young and aged mice.

**Results:** Our results show that after CM injection the dyes and conjugated antibodies accumulated at CP site. They were then transported via the lymphatic vessels through the nasal mucosa to the nasopharyngeal area of mice until they finally reached the cervical lymph nodes. Furthermore, aged mice showed a reduced lymphatic area at the CP side compared to their younger counterparts. Surprisingly, lymphatic vessels in the nasal mucosa lacked LYVE1 expression. VE-cadherin staining showed button-like junctions whereas smooth muscle coverage was absent.

**Conclusion:** Our results suggest that the lymphatics around the CP and in the nasal mucosa indeed represent one of the outflow routes of CSF. The reduced lymphatic coverage at the CP site is in agreement with previous findings of reduced lymphatic outflow capacity in aged mice. While lymphatics in the nasal mucosa did not express LYVE1, they showed characteristics of initial lymphatics such as button like junctions and lack or scarcity of vascular smooth muscle coverage.

## P 15

## De novo expression of immunomodulatory molecules on the endothelium controls tumor growth and metastasis

*E. Biglieri, S. Rotter, L. Borsig (Zürich)*

**Objective:** Metastasis is primarily responsible for the morbidity and mortality of cancer. Crosstalk between tumor cells and the local microenvironment is crucial for the outcome of metastasis. Especially the interaction between endothelial cells and tumor cells is essential for extravasation and metastatic progression. However, the precise role of endothelial cells in organ specific metastasis remains poorly understood. Overall, our aim is to study the contribution of the microvascular endothelium to metastasis and identify potential endothelial derived factors essential for liver and lung metastasis.

**Methods:** We analyzed RNA transcriptomes of activated endothelial cells from metastatic foci at two different sites (lung and liver), using three different spontaneous metastatic mouse models. Bioinformatic tools were used to determine common pathways involved in lung and liver endothelial cell activation, and protein-protein interaction networks identified targets which are upregulated and highly interconnected in endothelial cells of metastatic origin.

**Results:** We identified a member of the TNF receptor family to be specifically upregulated on endothelial cells within metastatic foci, while no expression was detected in adjacent lung tissue. Endothelial-specific deletion of this co-stimulatory immune checkpoint molecule resulted in enhanced spontaneous lung metastasis. Furthermore, we observed changes in lymphocyte infiltration, both in primary tumors and in metastatic lesions.

**Conclusion:** Overall, our study discovered novel endothelial cell-derived factors which are potentially involved in lung metastasis. The analysis of RNA transcriptomes and protein-protein interaction revealed several interesting targets whose roles in metastasis will be further investigated.

## P 16

### Transcriptional Response of Lymphatic Endothelial Cells in Lymph Nodes to Inflammation

*E. Sibler[1], Y. He[1], L. Ducoli[1], N. Keller[1], N. Fujimoto[2], L. C. Dieterich[1], M. Detmar[1] ([1]Zürich, [2]Otsu JP)*

**Objective:** The lymphatic system, and lymph nodes (LNs) in particular, are important for effective immune responses, self-tolerance, and induction and resolution of inflammation. Lymphatic endothelial cells (LECs), which line the LN sinuses, play important roles in LN organization and the migration of immune cells into the LN parenchyma. In inflammation, the involved LNs and their LECs undergo drastic remodelling. Thus, we sought to investigate the transcriptional landscape of LN LECs in healthy and inflamed LNs.
**Methods:** Imiquimod-induced skin inflammation in mice was used as a model of the chronic immune-mediated disease psoriasis. We sorted individual LECs from fresh murine LNs draining either healthy or inflamed skin, and subjected them to single-cell RNA sequencing with Smart-Seq2.
**Results:** We identified previously described subsets of LECs, corresponding to specific anatomical locations within the LN. These subsets also showed differing transcriptional responses to inflammation in the tissue they drain. Among the differentially expressed genes we found CD200, which has been previously suggested as an immune regulator. CD200 was upregulated in the LECs of the subcapsular sinus floor on both the RNA and protein level in response to inflammation. Computational analysis of receptor-ligand pairs expressed on LECs and immune cells in the LN predicted numerous interactions between stromal and immune cells, highlighting the relevance of LECs for immune responses. Moreover, we compared our results with those of a recent study using an acute oxazolone-induced inflammation model, and found many genes to be consistently up- or down-regulated in LECs during inflammation.
**Conclusion:** Our study provides insights into the transcriptional regulation of LN LECs under physiological and inflammatory conditions. Our data suggest that the distinct subsets of LECs lining the LN sinuses have individual functions also in inflammation. Furthermore, LECs likely interact with immune cells in a multitude of ways, and there is considerable overlap in their response to different types of skin inflammation.

## P 17

### Cerebrospinal fluid outflow pathways at the cribriform plate along the olfactory nerves

*I. Spera[1], N. Cousin[2], M. Ries[2], A. Kedracka[2], M. Detmar[2], S. Proulx[1] ([1]Bern, [2]Zürich)*

**Objective:** Several studies showed that routes along the olfactory nerves that extend to the lymphatic vessels in the nasal submucosa are an important cerebrospinal fluid (CSF) outflow pathway. Previous evidence in our lab showed accumulation of fluorescent tracers at the cribriform plate, indicating the outflow has also occurred along the olfactory nerves. However, it is still unclear how the nerve sheaths connect to the lymphatic vessels and where the arachnoid barrier is breached. The aim of this study is to define anatomically the connections between the subarachnoid space (SAS) and the lymphatics at the exiting nerve routes.
**Methods:** We made use of Prox1-GFP reporter mice to visualize the lymphatic vessels. To identify the CSF outflow pathways, either pegylated (PEG) or unmodified microbeads have been infused intracerebroventricularly in Prox1-GFP mice. At 45 min after the infusion, mice were sacrificed, and a decalcification protocol was used in order to keep the bone structures of interest intact. Then, 20 um thick slices were obtained at the cryostat and imaging at the level of the cribriform plate was performed under either a fluorescence stereomicroscope or a confocal microscope. In some samples, immunofluorescence staining was performed by using E-cadherin antibody to detect the arachnoid barrier.
**Results:** As expected, unmodified microbeads remain stuck into the ventricles compared to the pegylated ones, therefore are not ideal to study the CSF outflow pathways. In the area immediately below the olfactory bulbs, where the olfactory nerves cross the cribriform plate, we observed PEG microbeads around the nerve bundles and in the lymphatic vessels crossing the cribriform plate. In addition, E- Cadherin staining revealed a discontinuous distribution of the arachnoid barrier at the midline under and between the olfactory bulbs.
**Conclusion:** These data showed that the PEG beads have a better drainage efficiency. Furthermore, our preliminary results indicate that there are direct and open connections from the CSF space to the lymphatic vessels crossing the cribriform plate and in the nasal submucosa, as particles of one micron diameter had access to the lymphatics. Supporting this conclusion, we did not observe beads in the submucosal interstitial tissue. Finally, the discontinuous distribution of the arachnoid barrier at this area could explain how the lymphatics get access to the SAS.

## P 18

### The role of core-1 derived O-glycans for the localization of Siglec-1-expressing macrophages

*J. Frey[1], M. D'Addio[1], P. Vonlanthen[1], S. Lambrinos[1], F. Brigger[1], C. Halin Winter[1], R. D. Cummings[2], M. Detmar[1], V. I. Otto[1] ([1]Zürich, [2]Boston USA)*

**Objective:** In the lymph node (LN), cellular interactions between macrophages and lymphatic endothelial cells (LECs) regulate macrophage localization and phenotype. The underlying mechanisms of these interactions are however poorly understood. Here, we investigate the potential role of sialylated O-glycans displayed by LN LECs for the interaction with Siglec-1 (CD169)-expressing macrophages.
**Methods:** To investigate the role of sialylated core 1-derived O-glycans on LECs, we generated a mouse line with a conditional, lymphatic-specific knockout of the T-synthase chaperone Cosmc (Cosmc fl/fl x PROX1:Cre-ERT2). The glycans present on primary murine LN LECs isolated from these mice were analyzed using lectin binding assays and mass spectrometry (MS). We furthermore performed in vitro adhesion assays involving wild type (WT) and Cosmc knockout LN LECs and macrophages from mice that express WT and a loss-of-(glycan-binding)-function mutant of Siglec-1 (Siglec-1 W2QR97A). We also quantified the Siglec-1 positive macrophages present in the LNs of Cosmc fl/fl x PROX1:Cre-ERT2 and Siglec-1 W2QR97A mice.
**Results:** While increased levels of Tn antigen were detected by lectin binding upon deletion of Cosmc in LN LECs, core-1 derived O-gly-

 

cans were not detectable by MS. Adhesion of macrophages to Cosmc knockout LN LECs was reduced compared to WT LN LECs. Similarly, macrophage adhesion to WT LN LECs was reduced upon loss of Siglec-1 function in macrophages. In vivo, the relative abundance of Siglec-1 expressing macrophages was significantly reduced upon both ablation of core-1 derived O-glycans on LECs and loss of the ability to bind sialic acids of macrophage-expressed Siglec-1.
**Conclusion:** Collectively, our data reveal a novel mechanism supporting the cellular interactions between macrophages and lymphatic endothelial cells (LECs) in the mouse LN: Sialylated O-glycans displayed on LN LEC provide binding sites for Siglec-1-expressing macrophages.

**P 19**

## Specific epigenetic modifications of lymphatic endothelial cells from human psoriatic skin lesions: New targets for anti-inflammatory therapy?

*J. Kim[1], C. Tacconi[1,3], Y. He[1], L. Pellaux[1], E. Sibler[1], G. Restivo[1], M. Drach[1], M. Levesque[1], A. Navarini[1,2], M. Detmar[1] ([1]Zurich, [2]Basel, [3]Milan IT)*

**Objective:** Psoriasis is a chronic inflammatory skin disease characterized by hyperproliferation of keratinocytes, inflammatory cell activation and remodeling of the vasculature. Importantly, even after successful therapy, skin lesions often recur at the same sites as the previously healed lesions, indicating a potential epigenetic memory of skin cells. Lymphatic vessels (LVs) play pivotal roles in the control of inflammation by draining immune cells, inflammatory cytokines and antigens away from the inflamed tissue. In psoriatic skin lesions, LVs are enlarged with impaired draining function. The aim of study is to investigate potential functional, transcriptional and epigenetic alterations of psoriatic LVs.
**Methods:** We isolated lymphatic endothelial cells (LECs) from both healthy skin and from lesional skin of psoriasis patients. Psoriatic LECs were investigated by phenotypic differences and RNA-sequencing. We next screened a library of 48 small molecular epigenetic modifier drugs for their potential to reduce the expression of these genes in psoriatic LECs.
**Results:** Psoriasis-derived LECs displayed enhanced tube formation even after several passages in vitro. RNA-sequencing revealed 6 genes that were significantly up-regulated in psoriatic LECs and that were also related to vascular development and morphogenesis by Gene Ontology analysis. By epigenetic modifier drug screening, we found that a specific BET family inhibitor consistently reduced the 6 target genes and also diminished tube formation specifically in psoriatic LECs but not in healthy skin-derived LECs. BRD4, encoding for bromodomain-containing protein 4, was significantly upregulated in psoriatic LECs and systemic treatment with a specific inhibitor of BRD4, using the imiquimod-induced psoriasis mouse model, significantly reduced inflammatory ear swelling, the PASI (Psoriasis Area and Severity Index) score and also the weight of the draining lymph node.
**Conclusion:** These data indicate that LECs in chronic inflammatory skin lesions undergo epigenetic modifications that impact their transcriptional and functional activities, and that epigenetic re-programming might be a promising new approach for the treatment and/or prevention of relapse of chronic inflammatory diseases.

**P 20**

## A murine model for investigating the circulation and efflux of cerebrospinal and brain interstitial fluid after intracerebral hemorrhage

*A. Madarasz, S. Proulx (Bern)*

**Objective:** Intracerebral hemorrhage (ICH) is responsible for 10–15% of all observed strokes and is associated with high disability and mortality rates. Even patients that survive the critical postictal hours, might die as a result of brain edema formation and elevated intracranial pressure (ICP) with associated complications and concomitant brain damage. Most therapeutic approaches lack broad agreement and thorough validation, especially for the reduction of brain edema. The current literature suggests brain interstitial fluid (ISF) efflux along white matter tracts and perivascular spaces around blood vessels. Clinical studies have shown an accumulation of fluid in perivascular spaces of the brain after ICH; therefore, we consider diminished ISF clearance as a possible contributing factor to persistent brain edema after ICH. Moreover, as a consequence of an increased ICP, we expect an impaired efflux of cerebrospinal fluid (CSF) along perineural routes of cranial nerves to the cervical lymphatics. Our aim is to establish a model for in vivo studies of ISF and CSF circulation and efflux after intracerebral hemorrhage in mice.
**Methods:** Our experiments are performed in Prox1-EGFP and NG2-DsRed double transgenic mice that enable us to visualize the lymphatic endothelium as well as vascular pericytes. We assess CSF and ISF circulation and efflux in vivo using biologically inert near-infrared (NIR) tracers injected into the cisterna magna or lateral ventricles following ICH induction by collagenase VII-S injection into the caudoputamen. Brain vascular structure and hematoma size as well as erythrocyte spread are quantified using fluorescence microscopy.
**Results:** Our pilot experiments indicate differences in ICH hematoma size and expansion depending on the time of survival after ICH induction. Moreover, our results suggest a spread of erythrocytes from the center of hemorrhage to the perivascular spaces of surrounding arteries. First pilots show the feasibility of in vivo imaging of tracer circulation and efflux after ICH induction.
**Conclusion:** Here we present a novel approach for studying ISF and CSF circulation after ICH using double transgenic reporter mice enabling us to visualize arterial vessels in the brain with surrounding extravascular erythrocytes as well as in vivo NIR tracer efflux to the cervical lymphatics.

**P 21**

## Beyond pericytes – PDGF-BB accelerates vascular stabilization by stimulating the Semaphorin3A/Neuropilin1+ monocyte axis.

*A. Banfi, E. Bovo, S. Reginato, E. Groppa, N. Di Maggio, A. Grosso, S. Brkic, R. Gianni-Barrera (Basel)*

**Objective:** Vascular Endothelial Growth Factor (VEGF) is the master regulator of angiogenesis. However its therapeutic potential is challenged by the need to control both the dose and duration of expression: high and sustained expression causes aberrant angiogenesis,

but sustained delivery for at least 4 weeks is required for new vessel persistence. Accelerating new vessel stabilization would enable transient and safe VEGF delivery. We previously found that: 1) high VEGF doses impair vessel stabilization by inhibiting the endothelial Semaphorin3A (Sema3A)/Nrp1+ monocytes (NEM)/TGF-b1 paracrine axis; and 2) Platelet-Derived Growth Factor-BB (PDGF-BB) co-expression restores normal angiogenesis despite high VEGF levels. Here we investigated whether and how PDGF-BB accelerates the stabilization of VEGF dose-dependent angiogenesis.

**Methods:** Mouse leg muscles were implanted with monoclonal populations of genetically modified myoblasts homogeneously producing specific VEGF levels that cause normal (low and medium) or aberrant angiogenesis (high), alone or with a fixed 1:3 ratio of PDGF-BB (V+P). VEGF signaling was abrogated by systemic treatment with the receptor-body Aflibercept after 2 or 3 weeks.

**Results:** Increasing VEGF doses progressively impaired stabilization. PDGF-BB did not modify low and medium VEGF effects, but it greatly accelerated vascular stabilization with high VEGF (95% at 3 weeks vs 0% with VEGF alone). All normal capillaries induced by different V or V+P doses displayed similar pericyte coverage and functional perfusion, despite different stabilization rates. However, PDGF-BB co-expression restored Sema3A production, NEM recruitment and TGF-b1 levels in vivo despite high VEGF, leading to endothelial quiescence. PDGF-BB directly increased Sema3A expression dose-dependently in vivo even without VEGF. Blockade of Sema3A/Nrp1 binding abolished NEM recruitment and greatly reduced vessel stabilization by both V and V+P. In vitro VEGF and PDGF-BB had direct and opposing effects on endothelial Sema3a. Co-expression prevented VEGF-induced loss of Sema3a both in vitro and in ex vivo-isolated endothelium. In situ hybridization revealed that PDGF-BB specifically and dose-dependently expanded a non-endothelial source of Sema3A expression.

**Conclusion:** We identified a novel role for PDGF-BB to promote vascular stabilization independently from pericyte recruitment, by regulating the Sema3A/NEM/TGF-b1 axis.

## P 22

## Dynamic microvasculature-on-chip: breathing motions and vascular remodeling in vitro

*S. Zeinali, e.K. Thompson, T. Geiser, O.T. Guenat (Bern)*

**Objective:** In blood vessels, endothelial cells are exposed to mechanical stimuli, in particular cyclic strain present in organs, such as the lung. Mechanical stress creates evident physiological, morphological, biochemical, and gene expression changes in the cells exposed to that. However, the exact mechanisms of mechanical signal transduction into biological response remain to be clarified. Identification of pathways involved in these processes might help elucidate novel mechanisms involved in vascular diseases. Existing in vitro models used to investigate the effect of mechanical stretch on endothelial cells are usually limited to two-dimensional (2D) cell culture platforms and poorly mimic the typical three-dimensional aspect of the microvessels. Here, we present a functional organotypic human vasculature model that allows studying the effects of 3D mechanical cyclic stretch) on vascular remodeling and endothelial cell morphology.

**Methods:** A multilayer platform is used to generate a 3D vessel in the middle of the hydrogel layer. Following the creation of the cylindrical cavity within the gel layer, endothelial cells are seeded through access reservoirs. After the formation of the confluent vessel wall, different magnitudes of the negative pressure are applied to the membrane and transferred to the gel layer incorporating the 3D vessel. The vessel is exposed to mechanical cyclic stretch resembling respiratory motions for 24 hours and the effect of mechanical cyclic stretch on the vascular remodeling in vitro is investigated.

**Results:** We showed that endothelial cells respond differently when exposed to different magnitudes of cyclic stretch. Furthermore, cyclic stretch increases endothelial barrier integrity, decreases angiogenic sprouting, reorients the cells, and decreases vascular barrier leakage.

**Conclusion:** Advanced microvasculature-on-chip models need to mimic the in vivo environment, including the crucial biomechanical and biochemical cues. Our in vitro dynamic vasculature platform represents a powerful method that allows the investigation of cyclic stretch effects on real vessels and enables the identification of the role and function of individual parameters of the cell culture that is not possible in animal models.

## P 23

## Identification of brain vascular cell-cell interactome in health and in Alzheimer's disease

*S.-F. Huang, A. Keller (Zürich)*

**Objective:** Blood flow regulation in response to neuronal activity takes place at the neurovascular unit (NVU). Dysregulated cell-cell communication at the NVU leads to vascular dysfunction and neurological disorders. The cerebral vascular tree is heterogeneous with distinct zones -arterial, capillary, venous – formed by specific cell types. It is likely that the cell-cell communication at the NVU differs along the vascular tree during physiology and diseases. Here, we aim to establish a comprehensive vascular cell-cell interactome.

**Methods:** We catalogued potential cell-cell interactions, and cell-matrix interactions at the NVU using publicly available single-cell/nuclei RNAseq dataset, NATMI (Network Analysis Toolkit for Multicellular Interactions) algorithm and g:Profiler. We explored a mouse brain vascular single-cell dataset that has 10 distinct vascular associated cell types, including three different endothelial (EC) subtypes (arterial, capillary, venous), pericytes, astrocytes, smooth muscle cell (SMC) subtypes, perivascular macrophages (PVMs) and perivascular fibroblasts (PVFs). Ligand-receptor pairs were mapped. Using the human Alzheimer's disease database, we further identified the region-specific alterations (hippocampus and cortex) at capillary.

**Results:** The interactome showed differences along the arteriovenous axis of the mouse dataset. We observed that astrocytes and PVMs primarily mediated autocrine interactions. More than 50% of PVF ligands could potentially interact with SMC, suggesting PVFs could modulate SMC function. EC ligands in arterioles and venules showed a different preference in interacted cell types. Even though ECs along the arteriovenous axis have similar enriched pathways, the molecular composition was distinct. In particular, arterial and venous ECs have similar blood flow regulatory molecules such as endothelin-1 and CD38, whereas capillary ECs present a different geneset. In AD brains, the cell-extracellular matrix (ECM) was the most prominent change at capillaries. Altered ECM paired integrins suggest a direct impact on cell behavior and vascular function.

**Conclusion:** The division of labor of the cerebral vasculature is highly complex. Our in-depth analysis gives insights into the cellular signaling network at the NVU. It will serve as a resource aiding the identification of pathological alterations in NVU cell-cell interaction.

## P 24

### Notch4 signaling regulates the outcome of intussusceptive/splitting angiogenesis by VEGF

*A. Uccelli[1], S. Pezzini[1,2], A. Capponi[1], B. Fogli[1], P.S. Briquez[3], J.A. Hubbell[3], A. Banfi[1], R. Gianni-Barrera[1] ([1]Basel, [2]Bologna IT, [3]Chicago USA)*

**Objective:** Vascular endothelial growth factor-A (VEGF) is the master regulator of vascular growth and a key target for therapeutic angiogenesis. However, VEGF causes either normal or aberrant angiogenesis depending on its dose in the microenvironment around each producing cell in vivo. We previously found that therapeutic doses of VEGF do not induce angiogenesis in skeletal muscle by the well-studied mechanism of sprouting, but rather through intussusception/splitting, whose regulation is essentially unknown. Notch signaling is critical in sprouting angiogenesis and endothelium expresses both Notch1 and Notch4. We previously found that Notch1 activation is lost during the transition between normal or aberrant angiogenesis by VEGF. Here we investigated whether and how Notch4 regulates the process of splitting angiogenesis by increasing VEGF doses, in the therapeutic target tissue of skeletal muscle.
**Methods:** Different VEGF doses, inducing normal or aberrant angiogenesis, were delivered in hindlimb skeletal muscles of SCID mice, by implanting well-characterized monoclonal populations of transduced myoblasts, or Notch4-KO mice, by either (i) fibrin matrices decorated with an engineered, cross-linkable version of VEGF protein or (ii) a therapeutically relevant adenoviral vector. Notch signaling was globally inhibited in SCID mice by co-expressing a secreted form of the ligand Dll4 (sDll4).
**Results:** In SCID mice, global Notch inhibition by sDll4 did not impair normal angiogenesis, but completely prevented aberrant vascular growth, converting it to morphologically normal and functionally perfused microvascular networks. The same results were observed when only Notch4 was abrogated in Notch4-KO mice without interfering with Notch1 signaling, both with controlled VEGF delivery in fibrin matrix and uncontrolled delivery with a clinically relevant adenoviral vector. The lack of Notch4 signaling did not affect the total amount of proliferating endothelial cells, but it significantly reduced their speed of proliferation, leading to a more moderate degree of circumferential enlargement and therefore enabling successful splitting into normal vascular structures.
**Conclusion:** Notch4 signaling determines the switch between normal and aberrant angiogenesis by modulating the speed of endothelial proliferation by VEGF. It is a relevant target to ensure therapeutic angiogenesis.

## P 25

### Sodium thiosulfate limits the development of intimal hyperplasia in human vein segments and in a mouse model of carotid stenosis.

*D. Macabrey, M. Lambelet, A. Longchamp, J.-M. Corpataux, F. Allagnat, S. Déglise (Lausanne)*

**Objective:** Bypass surgeries and other endovascular approaches to treat arterial occlusive diseases suffer from limited long-term patency due to re-occlusive vascular adaptations, a process called intimal hyperplasia (IH). IH develops in response to vessel injury, loss of endothelial cells (EC), leading to inflammation, dedifferentiation and proliferation of vascular smooth muscle cells (VSMC). Hydrogen Sulfide ($H_2S$) is an endogenously produced gas, with anti-oxidant and anti-inflammatory properties. In rodent models, the $H_2S$ salt sodium hydrogen sulfide (NaHS) reduces IH, and vascular patients have reduced circulating $H_2S$ levels. Here, we tested the therapeutic potential against IH of the clinically approved thiol source sodium thiosulfate (STS) in human vein segments obtained from vascular patients and in a mouse model of IH.
**Methods:** Human veins segments obtained from patients undergoing lower bypass surgery maintained in culture ex-vivo for 7 days to stimulate IH were treated with NaHS or STS. Mouse subjected to carotid artery stenosis to stimulate IH were treated systemically with NaHS or STS. IH was measured by histomorphology and VSMC proliferation measure by proliferating cell nuclear antigen (PCNA). In addition, primary human vascular smooth muscle cells (VSMC) were exposed in-vitro to the same $H_2S$ donors. Migration and proliferation of these primary cells were measured using a wound healing assay and BrDU incorporation, respectively. To assess cytoskeletal organization, tubulin and actin fluorescent stainings were performed on VSMC.
**Results:** STS and NaHS similarly prevented the development of IH in human vein segments ex-vivo and in carotids in vivo. PCNA staining of human veins or mouse arteries suggest that the $H_2S$ donors reduce IH by inhibiting VSMC proliferation. In vitro, STS and NaHS similarly inhibited migration and proliferation of primary VSMC. Immunofluorescent stainings of cytoskeletal proteins revealed that STS acts by interfering with microtubules organization.
**Conclusion:** Currently, there is limited strategy to reduce IH. STS treatment may be a new therapeutic strategy to limit VSMC proliferation, thereby reducing the development of IH.

## P 26

### The role of macrophage-derived Vascular Endothelial Growth Factor in adrenal gland homeostasis, ion balance and blood pressure control

*M. Karakone, C. Stockmann (Zürich)*

**Objective:** In addition to the complex interplay between the renal, endocrine and cardiovascular system, the involvement of immune cells in blood pressure control is increasingly recognized. Particularly macrophages fulfill previously unrecognized organ-specific functions that contribute to whole-body homeostasis under physio-



 

logic conditions. Macrophages release VEGF and its neutralization can have multiple effects on the different components of the vasculature, ranging from vascular rarefaction to more subtle changes like basement membrane alterations or perturbation of angiocrine signaling. Noteworthy, the adrenal gland cortex is characterized by high VEGF expression as well as sinusoidal vessels with a discontinued, fenestrated endothelium and the preservation of this vascular phenotype is likely to be a prerequisite for proper adrenal gland function.

**Methods:** Myeloid cell-specific knockout of VEGF was achieved by breeding male mice homozygous for the floxed VEGF allele with female mice (C57Bl/6J) homozygous for the floxed VEGF allele expressing Cre recombinase driven by the lysozyme M promoter (LysMCre+/VEGF+f/+f). For our studies, we used female mice at the age of 12 weeks or older carrying two floxed VEGF alleles and positive for cre-expression designated as mutants (Mut), whereas female littermates negative for cre expression (LysMCre-/VEGF+f/+f) served as wildtype controls (WT).

**Results:** Strikingly, in our preclinical studies, female mice with a myeloid cell-specific deletion of VEGF (VEGF/LysM cre mice) develop hypertension, along with decreased levels of potassium at the age of 12 weeks (but not before), hence, symptoms that indicate primary aldosteronism. This is associated with decreased vascular density, deposition of collagen I, thickening of the collagen IV + vascular basement membrane and increased aldosterone synthase expression in the zona glomerulosa in the adrenal gland. Moreover, immunohistochemistry staining performed on human adrenal adenoma slides reveals increased deposition of collagen I and collagen IV.

**Conclusion:** We hypothesize, that macrophage-derived VEGF is critically involved in vascular maintenance in the adrenal gland as well as in the pathophysiology of primary aldosteronism.

## P 27

## Hypoxic Natural Killer cells mediate a trade-off between angiogenesis and antibacterial defence during cutaneous wound healing

*M. Sobecki, E. Krzywinska, S. Nagarajan, L. Sommer (Zürich)*

**Objective:** During skin injury, immune response and regenerative angiogenesis have to be coordinated for rapid skin regeneration and the prevention of microbial infections. Hypoxia is a characteristic feature of the tissue microenvironment during skin repair and bacterial infections, with tissue oxygen tensions lower than 10 mmHg in wounds and necrotic tissue foci. Natural Killer (NK) cells infiltrate hypoxic skin lesions and Hypoxia-inducible transcription factors (HIFs) mediate adaptation to low oxygen. However, the significance of hypoxic NK cells for skin repair and antimicrobial defence remains unknown.

**Methods:** To test the role of the HIF pathway in NKp46+ cells during wound healing and bacterial infections, we performed 6 mm circular back skin punch biopsies on the back skin of mice and bacterial infections with a strain of the Gram-positive pathogen group A Streptococcus on mice with an in vivo, targeted deletion of HIF1-α as well as the negative HIF regulator von Hippel-Lindau (VHL) protein, specifically in NK cells via crosses of the loxP-flanked Hif1a allele and the loxP-flanked Vhl allele to the Ncr1 (NKp46) promoter-driven Cre recombinase, specific to NKp46-expressing innate lymphoid cells, including NK cells (resulting in Hif1αfl+/fl+/Ncr1cre+ mice, termed HIF1-α KO and Vhlfl+/fl+/Ncr1cre+ mice termed VHL KO).

**Results:** We demonstrate that mice lacking the Hypoxia-inducible factor (HIF)1-α isoform in NK cells show impaired release of the cytokines Interferon (IFN)-γ and Granulocyte Macrophage – Colony Stimulating Factor (GM-CSF) as part of a blunted immune response. This accelerates skin angiogenesis and wound healing but facilitates bacterial translocation across the vasculature. Despite rapid wound closure, bactericidal activity and the ability to restrict systemic bacterial infection are impaired. Conversely, forced activation of the HIF pathway slows down wound angiogenesis, supports cytokine release and NK cell-mediated antibacterial defence despite delayed wound closure. Our results identify, HIF1-α in NK cells as a nexus that balances antimicrobial defence versus angiogenesis and global repair in the skin.

**Conclusion:** Conceptually, this suggests that adequate antimicrobial defence in the skin is achieved at the expense of a limited vascular remodeling and repair, whereas an acceleration of wound angiogenesis comes with a lower guard against infections.

## P 28

## Automated analysis of T cell interactions with an in vitro model of the blood-brain barrier under physiological flow

*M. Vladymyrov, L. Marchetti, S. Aydin, S. Soldati, A. Ariga, B. Engelhardt (Bern)*

**Objective:** The endothelial blood-brain barrier (BBB) rigorously controls T cell trafficking into the central nervous system. Mouse and human derived brain microvascular endothelial cells (BMECs) are a powerful in vitro model to study the multi-step T cell extravasation across the BBB under physiological flow employing live cell imaging using differential interference or phase contrast microscopy. Previously available automated tools are not able to reliably differentiate T cells on top of the BMEC monolayers in the grayscale time-lapse datasets obtained in this modality, demanding primarily manual analysis.

Here we present a fully automated T cell migration analysis pipeline for multi-step T cell migration across BMEC monolayers under physiological flow in vitro.

**Methods:** To segment the T cells on top of the BMEC monolayers in the grayscale phase contrast time-lapse datasets we have employed 2D+T U-Net like fully convolutional neural networks for multitask learning. To account for cells migration in different regimes and under changing flow conditions we developed a flexible tracking based on global optimization. We have also optimized the acquisition pipeline to increase the acquired statistics.

**Results:** We demonstrate the performance of the pipeline based on the analysis of a 20 datasets. We show that the results confirmed of the automated measurement agree with manual analysis and previous studies.

**Conclusion:** This automated pipeline enables scalable investigation of T cell migration across the in vitro BBB model in an unbiased way. Additionally it enables gaining more insight on the behavior of individual T cells and their interaction with individual endothelial cells.

## P 29

### Ain't nothing but a heartbreak: Effects of chronic hypoxia on ischemic injury response in microvascular cardiac endothelial cells and fibroblasts

*J. Montgomery, O. Rusiecka, S. Morel, B. Kwak (Geneva)*

**Objective:** Ischemic heart disease is the leading cause of death worldwide. Previous studies have found that reducing connexin43 (Cx43) expression or inhibiting Cx43 channel function improves the outcome of cardiac ischemia/reperfusion (I/R) in healthy mice, but the effect of common comorbidities, such as chronic obstructive pulmonary disease, remains unexamined. The goal of this study was to determine the effects of chronic hypoxia on acute I/R events in Cx43 and its alternative translation fragment GJA1-20k in microvascular cardiac endothelial cells (MCECs) and primary cardiac fibroblasts (CFs).
**Methods:** MCECs or CFs were subjected to 3 days of normoxia or hypoxia prior to an acute oxygen/glucose deprivation (OGD) event lasting 30 min. Total cellular protein, total cellular RNA, or mitochondrial protein were then collected from the cells and compared against normoxic and hypoxic controls.
**Results:** Exposure to chronic hypoxia in MCECs reduced Cx43 mRNA ($p<0.001$; N=3), Cx43 ($p<0.05$), and GJA1-20k ($p<0.05$; N=5) protein expression. Normoxic MCECs exposed to OGD demonstrated slight increases in Cx43 mRNA ($p<0.05$; N=3) reflected in a notable doubling of the amount of GJA1-20k present in the cells ($p<0.05$; N=5) but no change in Cx43. While the dramatic change in Cx43 and GJA1-20k expression in whole cell lysates during chronic hypoxia was reflected in the mitochondria (Cx43:$p<0.05$; GJA1-20k:$p<0.01$; N=4), there was no response to short term OGD events. CFs responded differently; GJA1-20k protein expression was not altered during OGD, but instead full-length Cx43 was increased ($p<0.05$; N=5) and mRNA trended upwards ($p=0.06$; N=3). Chronic hypoxia in CFs did not alter full-length Cx43, but lowered the amount of GJA1-20k present ($p<0.05$; N=5). In both cell types, chronic hypoxia eliminated Cx43-related changes seen in normoxic cells during OGD.
**Conclusion:** Acute I/R-induced changes in GJA1-20k appear to be cell-type specific, occurring in microvascular cells outside the mitochondria but not in cardiac fibroblasts. Exposure to chronic hypoxia reduced baseline GJA1-20k present in cells and mitochondria, and prevented I/R-related GJA1-20k upregulation in MCECs and Cx43 full-length protein upregulation in CFs. Enhancing our knowledge of the effects of comorbidities on acute I/R events may help to better adapt cardioprotective treatments to specific patient groups.

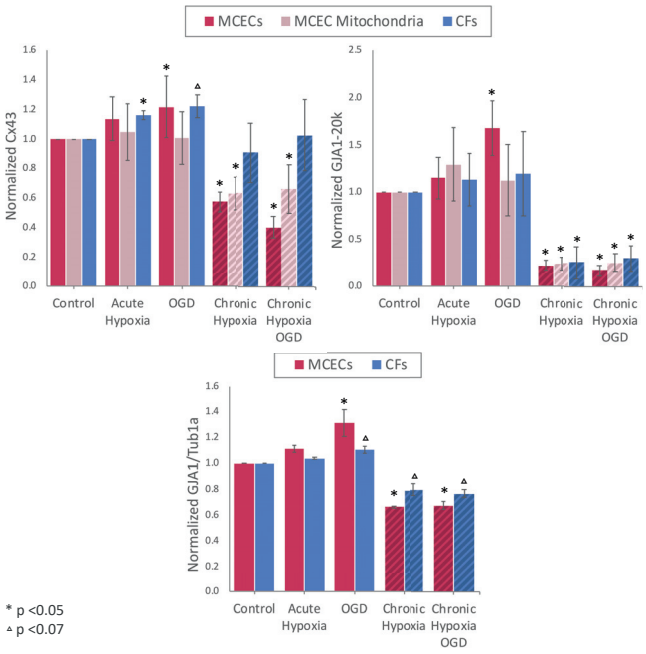


**Figure 1.** Different Cx43-related changes with ischemia (OGD) and chronic hypoxia (CH) were found among the cell types and organelles tested. In all cases there was no difference between CH and CH OGD conditions, suggesting that CH abrogates the normal Cx43-related response to ischemic injury.

## P 30

### Endothelial control of adipose tissue expansion

*L. Wetterwald, A. Köck, S. Arroz-Madeira, B. Prat-Luri, B. Haym, T. Berg, V. Zufferey, M. Delorenzi, A. Sabine, T.V. Petrova (Lausanne)*

**Objective:** Adipose tissue is a major player of metabolic homeostasis. Its dysfunction is tightly linked to pathologies such as obesity, insulin resistance, cardiovascular disease, and cancer. In the highly vascularized white adipose tissue endothelial cells fulfill multiple roles such as lipid transport, satisfying adipose tissue metabolic demand through angiogenesis and providing a niche for adipocyte progenitor cells. How endothelial cells govern the perivascular niche and adipose tissue expansion is incompletely understood.
**Results:** In this project, we identified the endothelial transmembrane adaptor protein Myct1 as a regulator of adult white adipose tissue expansion through the paracrine regulation of the perivascular niche. We apply now a combination of in vitro and in vivo analyses to decipher the molecular mechanisms underlying adipose-tissue specific functions of Myct1.
**Conclusion:** This study will deliver important fundamental knowledge about the vascular control of adipose tissue expansion and may suggest actionable targets for therapeutic intervention.

# Vascular surgery

## FM 4

### Stent Assisted Balloon Induced Intimal Disruption and Relamination (STABILISE) in Aortic Dissection Repair : a single-center observational study

*I. Sokolik, C. Deslarzes, J.-M. Corpataux, S. Déglise (Lausanne)*

**Objective:** TEVAR has become the treatment of choice for complicated type B aortic dissection. However, patent false lumen remains a risk factor for aneurysmal degeneration in a majority of patients. The goal of the treatment should therefore also focus on aortic remodel-

 

ling and false lumen obliteration. This study reports the mid-term results of 14 patients treated by the STABILISE technique for aortic dissection in our institution.

**Methods:** The data from all consecutive patients who benefited from the STABILISE technique for aortic dissection in our Hospital between October 2014 and April 2021 were reviewed. Patients were followed with CT scan at 1, 6 and 12 months and yearly thereafter. The primary endpoint was the false lumen obliteration rate at 6 months. Secondary outcomes were technical success, reintervention and mortality rate and patency rate of target vessels.

**Results:** Among the 14 patients included, there were 10 male with a median age of 60 years old. Indications were type B aortic dissection with malperfusion in 9 patients and early aneurysmal degeneration in 4 cases. In the remaining case, there was a thoracic aneurysm following a type A aortic dissection, prior requiring an elephant trunk. In 7 cases, deployment of TEVAR was in zone 3 and in 5 cases a debranching of the left subclavian artery was necessary to land in zone 2. In the remaining 2 cases, left subclavian artery debranching and left carotid chimney was performed to land in zone 1. There were no intra-procedural complications. A total of 11 target visceral vessels (1 CT, 4 SMA, 6 renals) in 8 patients (57%) were stented through the struts of the dissection stent. The 30-day cumulative incidence of death, stroke, and paralysis/visceral ischaemia was 0%. During the mean follow up of 11 months, 3 patients (21%) required a re-intervention for 1 type Ia and 1 type Ib endoleak and for a carotid chimney stenosis. Primary target vessel stent patency was 100%. No deaths occurred. On the most recent CT scan, complete false lumen obliteration was observed in all patients (100%) all along the thoraco-abdominal aorta.

**Conclusion:** The STABILISE technique seems to be safe and effective to obtain durable false lumen thrombosis and aortic remodelling in aortic dissections with the need for visceral vessles stenting in around half of cases. Further studies and longer follow-up are required to to confirm these excellent preliminary results.

## FM 2.1

### Patient-specific computational fluid dynamic simulation for assessing hemodynamic changes following branched endovascular aneurysm repair: a pilot study

*C. Deslarzes[1], K. Tran[2], A. Mardsen[2], J. T. Lee[2], S. Déglise[1]*
*([1]Lausanne, [2]Stanford USA)*

**Objective:** This pilot study assessed the hypothesis that patient-specific computational fluid dynamic (CFD) modelling can detect aortic branch hemodynamic changes following branched endovascular aneurysm repair (bEVAR).

**Methods:** Patients who underwent bEVAR with the Jotec E-xtra Design for thoracoabdominal aortic aneurysms were retrospectively selected. Using open-source SimVascular software, pre- and post-operative aortic finite element volume meshes were constructed from CT imaging. Pulsatile in-flow conditions were derived and adjusted for patient-specific clinical variables. Outlet boundary conditions consisted of Windkessel models approximated from physiologic flow splits. Rigid wall flow simulations were then performed on pre- and post-operative models with equivalent boundary conditions. Computations were performed with an incompressible Navier-Stokes flow solver on a 72-core cluster. Pre- and post-operative hemodynamic parameters such as arterial pressure, flow rate, and time-averaged wall shear stress (TAWSS) were then compared using paired analysis

**Results:** Pre- and post-operative flow simulations were performed on 10 patients who underwent uncomplicated bEVAR with a total of 40 target vessels (10 celiac, 10 superior mesenteric, 20 renal stents). Compared to pre-operative values, bEVAR was associated with a decrease in peak renal artery pressure (116.8 ± 11.5 vs 112.8 ± 11.6 mmHg, p=.0001) and flow rate (13.7 ± 2.3 vs 12.9 ± 2.4 ml/s, p=.0006). The majority of renal branches (n=15, 85%) had a post-operative decline in peak pressure of at least 1 mmHg. No post-operative differences were observed in pressure or flow rates in the celiac or mesenteric arteries (p=.10-.55). Mean paravisceral aortic TAWSS values increased significantly (1.37 ± 0.54 vs 3.56 ± 1.41 dynes/cm2, p=.001), with all subjects achieving aortic TAWSS values within normal physiologic range post-operatively. Aortic branches had mean TAWSS within the physiologic range both pre- and post-operatively.

**Conclusion:** Changes in para-visceral aortic geometry after bEVAR is associated with a decrease in computationally estimated renal perfusion, without significant changes to celiac or mesenteric hemodynamics. Further CFD simulation-based studies are needed to assess whether changes in branch hemodynamics or configuration after bEVAR can predict loss of branch patency.

## FM 2.2

### Single centre experience with the GORE EXCLUDER® iliac branch endoprosthesis for endovascular iliac aneurysm repair

*S. Hofer, M. Furrer (Chur)*

**Objective:** Adequate sealing and preserving of the hypogastric artery in patients with iliac artery aneurysms can be achieved with endovascular strategies using iliac branch devices. The aim of this study was to examine short and midterm outcome using the GORE EXCLUDER® iliac branch endoprosthesis (IBE).

**Methods:** Between September 2015 and Oktober 2021 we implanted 70 IBE in 57 patients with aneurysm of the common iliac artery (CIAA), aneurysm of the hypogastric artery (HAA) or with Type IB endoleak after previous endovascular aortic repair (EVAR). Postoperative outcome was assessed by CT scan on day one, day 90 and thereafter once yearly after surgery.

**Results:** In thirteen of the included 57 patients we performed a bilateral repair by IBE. Indications for IBE were a CIAA in 40 repairs, a HAA in seven patients and a combination of CIAA and HAA in thirteen patients. A type IB endoleak was sealed by IBE in 8 patients. In 27 cases we implanted IBE without an aortic extension. 17 patients presented with an iliac aneurysm harbouring additionally an aortic aneurysm requiring treatment. In thirteen cases we implanted the IBD after previous EVAR. A technically successful endovascular repair was performed in 65 cases (93%). A conversion to open repair was necessary in three patients, one due to stentgraft dislocation, one with mycotic aneurysm and one because of aortic anerysm sac growth and Typ I A endoleak. Two patients showed an early occlusion of the hypogastric artery (3%). Early reintervention was required in eight patients due to four stentgraft stenoses, three endoleak type I and one stentgraft dislocation.

During a mean follow-up time of 24 months (range 0–69 months) the patency rate was 100% . A reintervention during follow-up time was

performed in four patients, (5.7%) two because of an endoleak type I after 42 months and two because of endoleaks type III after 3 and 27 months. Sac shrinking could be achieved in 46, sac stabilisation in 12 aneurysms . No buttock claudication occurred.

**Conclusion:** Using an IBE is an effective and safe option for CIAA and HAA, avoiding complications asssociated with intentional occlusion of internal iliac artery. Short and midterm outcome shows a very good patency and a low complication rate.

## FM 2.4

### Initial experience using pericardial patches as arterial tube grafts in below-the-knee revascularization

*E. Côté, J. Longchamp, Y. De Leon, A. Longchamp, R. Trunfio, J. Brusa, J.-M. Corpataux, S. Déglise, C. Deslarzes (Lausanne)*

**Objective:** Autogenous vein remains the conduit of choice for below-the-knee bypass but is not available in about 30% of cases. Alternatives such as cryopreserved vessels or prosthetic material are often limited by their availability, patency and resistance to infection. The aim of this study is to report the results of our preliminary experience using pericardial tube grafts in below-the-knee revascularization when there is no vein available.

**Methods:** From March 2020 to May 2021, we included 28 consecutive patients, operated in our Department for a below-the-knee bypass using either bovine pericardial pre-sewed tube grafts (Perima; BioModiVasc, Canada) or self-made porcine pericardial tube grafts (No-react; BioIntegral Surgical, Canada). Follow-up was performed with duplex ultrasound at 7 days, 1, 3, 6 and 12 months. The primary outcome was the secondary patency at 1, 3 and 6 months. Secondary outcomes were primary patency, survival, limb salvage and reintervention rates.

**Results:** Among the 28 patients (23 males, 82.1%) with a mean age of 73 years (range: 52–90), 22 (79%) suffered from arterial hypertension and 14 (50%) had a concomitant cardiac disease. Ten patients (36%) had a previous peripheral bypass. Indications for surgery were chronic arterial disease with Rutherford stages II-VI in 21 patients (75%) and acute ischemia in 7 (25%).

Pre-sewed pericardial patches were used in 18 (64%) patients and self-made tubes grafts in 10 (36%). The distal anastomosis was performed on the distal popliteal artery in 14 patients (50%) and on the tibial arteries in the other 14 (50%). Total procedure time was 184.2 minutes (range: 105–336). Mean hospital stay was 16.1 days (range: 2–63). One patient (4%) died within the hospital stay. During the mean follow-up of 86 days (range: 0–378), reintervention occurred in 22 (79%) patients, 12 (43%) for bypass occlusions, 3 (11%) for bypass bleeding and 7 (25%) for wound complications. Freedom from amputation was 75%.

Secondary patency rates at 1, 3 and 6 months were 70%, 64% and 50% respectively. Primary patency rates at 1, 3 and 6 months were 64%, 46% and 43% respectively.

**Conclusion:** The use of pericardial tube grafts seems to be a limited option for below-the-knee revascularization due to high reintervention rate and low patency rate. There is need for studies proposing new alternatives to help choosing the best conduit when no autologous material is available.

## FM 2.5

### Swiss multicenter observational study of the Gore Excluder Conformable endograft for endovascular abdominal aortic repair: initial results

*A. Roesti[1], S. Hofer[2], A. Isaak[3], G. Gemayel[4], E. Mujagic[5], L. Briner[6], T. Wolff[5], C. Deslarzes[1], J.-M. Corpataux[1], S. Déglise[1] ([1]Lausanne, [2]Chur, [3]Aarau, [4]Geneva, [5]Basel, [6]Neuchâtel)*

**Objective:** Endovascular repair (EVAR) has become the standard of care for the treatment of abdominal aortic aneurysms. However, a significant number of EVAR remains outside the IFU, especially in cases of severe proximal angulation (>60 degrees). The new device GORE EXCLUDER Conformable AAA Endoprosthesis (W.L. Gore & Associates, Flagstaff, Ariz) has been specifically designed to accommodate neck angulation, due to conformability and angulation control. This study aims to report the initial results of this device.

**Methods:** From March 2019 to January 2021, the data of all consecutive patients with AAA treated with the Gore Excluder Conformable endograft at 6 vascular centers were reviewed. Patients were followed using a standardized protocol, with CT-scan at 1, 6, 12 months, and then yearly. The primary endpoint was technical success and secondary outcomes were postoperative morbidity, rate of endoleak (EL) and any aneurysm-related re-interventions.

**Results:** Fifty-four patients were included, with a mean age of 76 y. The mean diameter of AAA was 62 mm (47–110). The mean length of the aortic neck was 26 mm (5–69), the mean diameter 23 mm (14–31) and the median neck angulation was 72 degree (32–150). Indication was hostile neck in all cases with severe angulation in 45 cases. In 3 cases, it was a redo (2 type Ia ELs, 1 neck dilatation). The mean procedural duration was 107 min (54–210) with a mean time of scopy of 25 min (7–66) and a total volume of contrast of 131 ml (40–340). Technical success was 96.3% with 2 type Ia endoleak (3.7%). In the post-operative period, 11 complications were observed (7 medical and 4 surgical). Three reinterventions (5.6%) were needed (1 iliac angioplasty, 2 corrections of femoral false aneurysm). The first angio-CT revealed 5 type Ia ELs. During the mean follow-up of 7 months (1–22), 3 type Ia Els spontaneously resolved, one was followed and the last one required an open conversion. One distal limb extension was implanted at 3 m for a type Ib EL with a total rate of reintervention of 9%. No migration and no death occured.

**Conclusion:** The use of the Gore Excluder Conformable endograft seems to be safe and effective in challenging anatomies and especially heavy aortic neck angulation. It allows for precise deployment without the need for additional contrast or operation time. Longer follow-up and more patients are required to confirm these excellent initials results.

## P 5

### Case report: Whoops resection in a leiomyosarcoma of the external iliacal vein

*E.L. Tobler, C. Kohler, S. Weiss, C. Ionescu, Y. Banz, M.K. Widmer (Bern)*

**Objective:** Venous leiomyosarcoma (LMS) is a rare soft tissue malignancy. Misdiagnosis of this entity may lead to a "whoops" procedure, which is the resection of a sarcoma without being aware of the diagnosis.
**Methods:** Case report of a patient with venous LMS who underwent a "whoops" procedure, describing the further therapeutic strategy.
**Results:** A 62-year-old female patient presented with swelling of the left leg. Imaging in various modalities showed a left pelvic tumor, which was classified as ovarian etiology. The patient underwent diagnostic laparoscopy at a tertiary gynecology center. Intraoperatively, both ovaries appeared without macroscopic pathological findings but a left retroperitoneal mass adjacent to the external iliac vein was observed. An intraoperative frozen section was collected. Definitive histopathology showed a venous LMS of the conventional type (R1 Whoops resection). Due to the possible peritoneal contamination by the laparoscopic tumor biopsy, an interdisciplinary decision was made to complete tumor resection by resecting the external iliac vein and replace it with a xenopericardial tube graft. Histopathology of this procedure showed remaining tumor cells in the resection margin. Thus, left adnexectomy combined with intraoperative radiation and extended resection of the proximal iliac vein with a new xenopericardial interposition graft was performed. Histopathologically, tumor-free resection margins were confirmed. 14 days later, the patient showed an early re-thrombosis of the femoral vein reconstruction, followed by an emergency venous thrombectomy and placement of an arterio-venous (AV) fistula. However, the venous xenopericardial tube again occluded without further surgical escalation followed. The patient was able to discharge with anticoagulation and compression stockings with leg edema still persisting. A follow-up consultation at 6 months showed a good general condition and MR imaging at 9 months revealed no evidence of recurrent leiomyosarcoma.
**Conclusion:** A "whoops" procedure for venous LMS may occur despite preoperative imaging and intraoperative frozen section examination. However, when occurred, an interdisciplinary approach is needed to define the further treatment strategy, including vein replacement. In this patient, a xenopericardial tube graft was used for venous reconstruction.

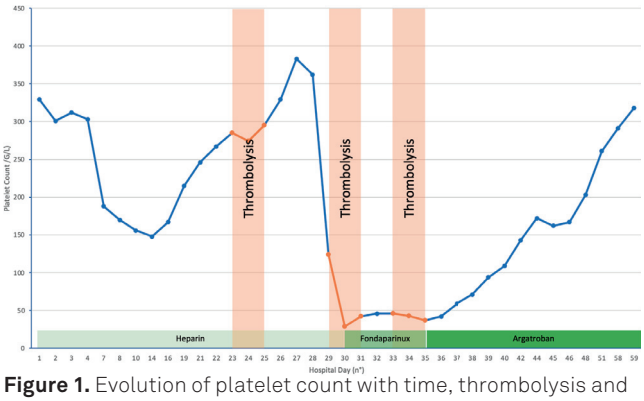


**Figure 1.** Evolution of platelet count with time, thrombolysis and anticoagulation.

## P 6

### In situ arterial thrombolysis in severe heparin-induced thrombocytopenia: a case report

*R. Varone (Sion)*

**Objective:** Severe thrombocytopenia is a relative contraindication for thrombolytic therapy. There are no clear guidelines addressing the use of thrombolysis to treat acute limb ischemia (ALI) in patients with heparin-induced thrombocytopenia (HIT). We report the case of one patient with ALI who, despite severe HIT (platelet count down to 29G/L), underwent repeated CDT with no bleeding side-effects.
**Methods:** We report the case of a 75-year-old, COVID-19 positive, man who on hospital day 23 presented a left ALI Rutherford grade IIa. A continuous CDT was started with Alteplase 1 mg/h as well as a continuous intravenous infusion of unfractionated heparin (UFH). CDT was stopped after 48 hours with complete clot lysis and UFH was continued. On hospital day 29, the patient presented a second left ALI with acute severe thrombocytopenia (down to 29G/L). CDT was repeated for 48 hours but at a lower dose (0.5 mg/h) with clinical recovery. Because of suspected symptomatic HIT type II, UHF was stopped and replaced by Fondaparinux. The platelet count stabilized at 45 G/L without further increase thereafter. On hospital day 33, the patient presented a third episode of ALI with bilateral femoro-popliteo-tibial thrombosis. As a Fondaparinux cross allergy was suspected, it was replaced by Argatroban. CDT was repeated once again, followed by satisfactory clinical improvement, then definitively stopped after two days. Follow up was uneventful thereafter, without any new thrombotic event. The right limb recovered without functional deficit but partial peripheral neurologic deficit persisted on the left limb. The patient died 3 months later due to a cardio-renal syndrome.
**Results:** Because of bleeding risks, physicians might restrain from treating ALI by thrombolysis if their patients suffer from HIT. However, only few published articles describe bleeding complications in such cases. In our case, despite a thrombocyte count down to 29G/L, three consecutive CDT did not lead to any bleeding complications.
**Conclusion:** The use of CDT to treat arterial thrombosis in HIT patients is reasonably safe despite very low platelet count. Further studies are required to establish clear guidelines for the use of thrombolysis in ALI and HIT.

## P 8

### Management of type A aortic dissection in a patient with right aortic arch and aberrant left subclavian artery with placement of an AMDS hybrid stent: A case report

*A. Roesti, A. Nowacka, J. Namasivayam, M. Sabour, D. Delay (Sion)*

**Objective:** Dissection of a right-sided aortic arch with aberrant left subclavian artery is a rare entity without consensus for gold standard treatment. Only few cases were described with different surgi-

cal strategies such as total arch replacement with TEVAR or frozen elephant trunk. Here we present a case of type A aortic dissection of right-sided aortic arch treated in an hybrid approach

**Methods:** A 49-year-old man was admitted to our hospital for acute chest pain with neck irradiation. Computed tomography (CT) demonstrated acute type A aortic dissection extending to descendant thoracic aorta in a right-sided aortic arch with aberrant left subclavian artery originating from Kommel's diverticulum (KD).

The patient underwent replacement of the ascending aorta (24 mm straight tube) and stenting of the aortic arch (40 mm hybrid AMDS stent) under extracorporeal circulation with cannulation of the right femoral artery and semi-selective cerebral perfusion through the left carotid artery.

**Results:** The postoperative course was uneventful. CT – scan on POD 5 revealed obliteration of the false lumen in the arch and in the distal descending thoracic aorta with persistent opacification of the false lumen of in front of the left subclavian artery probably related to a widening of the aorta due to KD, with a cross-sectional diameter at the origin of the left subclavian measuring less than 2 cm. The patient was discharged home on POD 11 and he remains well.

**Conclusion:** To our knowledge, there is no study describing right-sided aortic arch dissection treated with interposition graft of the ascending aorta and hybrid AMDS stent placement. Our case demonstrate a good intra-operativ and short-term result without increasing technical complexity. With think that this approach could represent an interesting alternative to the emergency management of this rare anatomical variation with good opening of the true lumen, reducing perfusion of the false lumen and stabilization of the aortic diameter without compromise of the perfusion of the supra-aortic trunks. Naturally close follow-up is necessary for long-term result.

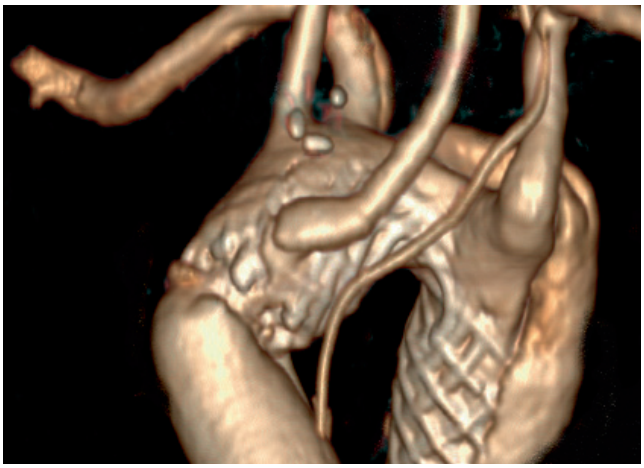

**Figure 1.** Post-operative CT-Scan.

# Autorenverzeichnis/Relevé des auteurs